Using the extended Melnikov method to study the multi-pulse global bifurcations and chaos of a cantilever beam

W. Zhang*, M.H. Yao, J.H. Zhang

College of Mechanical Engineering, Beijing University of Technology, Beijing 100022, PR China

Abstract

The aim of this paper is to investigate the multi-pulse global bifurcations and chaotic dynamics for the nonlinear non-planar oscillations of a cantilever beam subjected to a harmonic axial excitation and two transverse excitations at the free end by using an extended Melnikov method in the resonant case. First, the extended Melnikov method for studying the Shilnikov-type multi-pulse homoclinic orbits and chaos in high-dimensional nonlinear systems is briefly introduced in the theoretical frame. Then, this method is utilized to investigate the Shilnikov-type multi-pulse homoclinic bifurcations and chaotic dynamics for the nonlinear non-planar oscillations of the cantilever beam. How to employ this method to analyze the Shilnikov-type multi-pulse homoclinic bifurcations and chaotic dynamics of high-dimensional nonlinear systems in engineering applications is demonstrated through this example. Finally, the results of numerical simulation are given and also show that the Shilnikov-type multi-pulse chaotic motions can occur for the nonlinear non-planar oscillations of the cantilever beam, which verifies the analytical prediction.
© 2008 Elsevier Ltd. All rights reserved.

1. Introduction

Cantilever beams are flexible structures which are applied in many different engineering projects. The nonlinear non-planar dynamics of cantilever beams is the subject of interest because of their wide practicability in spacecraft stations, satellite antennas, machine tools, flexible manipulators and so on. Therefore, research works on the nonlinear non-planar dynamics of cantilever beams have received considerable attention in the past three decades. With the development of the theories of nonlinear dynamics and chaos, prediction, understanding and control become possible for flexible cantilever beams in a more complicated nonlinear phenomena such as the global bifurcations and the Shilnikov-type chaotic dynamics.

The global bifurcations and chaotic dynamics of high-dimensional nonlinear systems have been at the forefront of nonlinear dynamics for the past two decades. Many researchers have paid considerable attention to high-dimensional nonlinear systems [1,2]. There were many difficulties for studying the complicated dynamics of high-dimensional nonlinear systems. Compared to low-dimensional nonlinear systems, the results

*Corresponding author.

E-mail addresses: sandyzhang0@yahoo.com (W. Zhang), merry_mingming@emails.bjut.edu.cn (M.H. Yao).

of research on the complicated dynamic behavior of high-dimensional nonlinear systems were less in the early references. The governing equations of motion for many engineering problems can be described by high-dimensional nonlinear systems. It is noticed that the obtained high-dimensional nonlinear systems are also high-dimensional Hamiltonian systems with the perturbations. Therefore, the global bifurcations and chaotic dynamics of high-dimensional nonlinear systems are important theoretical problems in science and engineering applications as they can reveal the instabilities of motion and complicated dynamical behaviors. New complex phenomena on the global bifurcations and chaotic dynamics are discovered in high-dimensional nonlinear systems, such as the multi-pulse Shilnikov orbits.

Despite lack of analytical tools and methods to study the global bifurcations and chaotic dynamics for high-dimensional nonlinear systems, certain progress has been achieved in this field in the last two decades. Thorough investigations on the global bifurcations and chaotic dynamics of high-dimensional nonlinear systems are being conducted by researchers. In book [3], Wiggins gave a detailed classification on four-dimensional perturbed Hamiltonian systems and divided them into three basic types. He used the Melnikov method to investigate the global bifurcations and chaotic dynamics for these three basic systems. Based on the Wiggins' study in Ref. [3], Kovacic and Wiggins [4] developed a new global perturbation technique which may be utilized to detect the Shilnikov-type single-pulse homoclinic and heteroclinic orbits in four-dimensional autonomous ordinary differential equations and gave an application to the forced and damped sine-Gordon equation. This global perturbation technique is a combination of higher-dimensional Melnikov theory, geometrical singular perturbation theory and the theory of invariant manifolds. It is thought that this technique is fairly effective when the Shilnikov-type single-pulse homoclinic and heteroclinic orbits are studied in four-dimensional nonlinear systems. With the aid of new global perturbation technique, Kovacic [5] investigated the existence of the orbits homoclinic to resonance bands for Hamiltonian systems subjected to small amplitude Hamiltonian. Later on, Kovacic [6,7] utilized a combination of the Melnikov method and geometrical singular perturbation theory to, respectively, study the orbits homoclinic to resonance bands in a class of near-integrable Hamiltonian systems and the existence of the homoclinic and heteroclinic orbits in a class of near integrable dissipative systems.

Several researchers applied the aforementioned global perturbation technique to many engineering problems. Feng and Wiggins [8] employed the global perturbation technique to study the global bifurcations and chaotic dynamics for parametrically excited mechanical systems with $O(2)$ and $Z_2 \oplus Z_2$ symmetries. Feng and Sethna [9] utilized the global perturbation method to study the global bifurcations and chaotic dynamics of the thin plate under parametric excitation and obtained the conditions in which the Shilnikov-type homoclinic orbits and chaos can occur. Malhotra and Sri Namachchivaya [10] made use of the global perturbation method to analyze the global dynamics and chaos of parametrically excited nonlinear reversible systems with non-semisimple 1:1 resonance. Malhotra and Sri Namachchivaya [11] used the averaging method and Melnikov technique to study the local, global bifurcations and chaotic motions of a two-degree-of-freedom shallow arch subjected to simple harmonic excitation for the case of internal resonance. Feng and Liew [12] analyzed the existence of the Shilnikov-type single-pulse homoclinic orbits in the averaged equation which represents the modal interactions between two modes with zero-to-one internal resonance and influence of the fast mode on the slow mode. The zero-to-one internal resonance means that there are one non-semisimple double zero and a pair of pure imaginary eigenvalues in the averaged equation. The global bifurcations and chaotic dynamics were investigated by Zhang et al. [13] and Zhang [14] for both parametrically-externally excited and parametrically excited simply supported rectangular thin plates. In these researches, the method of normal form was utilized to reduce the averaged equation to a normal form which is a simpler form than the original system. Furthermore, Zhang and Li [15] employed the global perturbation approach to investigate the global bifurcations and chaotic dynamics for a two-degree-of-freedom nonlinear vibration absorber. Zhang and Tang [16] studied the global bifurcations and chaotic dynamics of the suspended elastic cable to small tangential vibration of one support which causes simultaneously the parametric excitation of the out-plane motion and the parametric and external excitations of the in-plane motion. Guo and Chen [17] used the global perturbation technique to analyze the Shilnikov-type single-pulse homoclinic orbit in a six-dimensional truncated system of perturbed nonlinear Schrodinger equation. Recently, Zhang et al. [18] utilized the global perturbation technique to investigate the Shilnikov-type single-pulse global bifurcations and chaotic dynamics for the nonlinear non-planar oscillations of the cantilever

beam. Cao and Zhang [19] employed the global perturbation method to investigate the Shilnikov-type single-pulse global bifurcations and chaotic dynamics in a string-beam coupled system.

Besides the aforementioned researches on the Shilnikov-type single-pulse global bifurcations and chaotic dynamics of high-dimensional nonlinear systems, several researchers also investigated the Shilnikov-type multi-pulse homoclinic and heteroclinic bifurcations and chaotic dynamics. In 1996, Kovacic and Wettergren [20] used a modified Melnikov method to investigate the existence of the multi-pulse jumping of homoclinic orbits and chaotic dynamics in resonantly forced coupled pendula. Furthermore, Kaper and Kovacic [21] studied the existence of several classes of multi-bump orbits homoclinic to resonance bands for completely integral Hamiltonian systems subjected to small amplitude Hamiltonian and damped perturbations. Camassa et al. [22] presented a new Melnikov method which is called as the extended Melnikov Method to investigate the multi-pulse jumping of homoclinic and heteroclinic orbits in a class of perturbed Hamiltonian systems. They gave a detailed mathematical proving procedure on the extended Melnikov method, which unifies several previously disjoint perturbation theoretical methods. From engineering and application point of view, it is thought that this method is too abstract and abstruse for engineering scientists. Therefore, no any engineering scientists utilized the extended Melnikov method to investigate the Shilnikov-type multi-pulse homoclinic and heteroclinic bifurcations and chaotic dynamics of high-dimensional nonlinear systems in engineering applications in the past several years.

In the meantime, the energy-phase method was first presented by Haller and Wiggins [23] where single-pulse orbits homoclinic to a resonance in the Hamiltonian case were studied in detail. Subsequently, Haller and Wiggins [24,25] further developed the energy-phase method to investigate the existence of the multi-pulse jumping of homoclinic and heteroclinic orbits in the damped-forced nonlinear Schrodinger equation and perturbed Hamiltonian systems. In Ref. [26], Haller and Wiggins utilized the energy-phase method to study the Shilnikov-type multi-pulse homoclinic and heteroclinic orbits and chaotic dynamics for three-degree-of-freedom Hamiltonian systems. Using the energy-phase method, Haller [27] studied the *n*-pulse homoclinic and heteroclinic orbits in multimode truncated and discretized dynamical system of the perturbed nonlinear Schrodinger equation. In book [28] published by Haller in 1999, he summarized the energy-phase method and presented detailed procedure of application to several problems in mechanics, which include the Shilnikov-type multi-pulse homoclinic and heteroclinic bifurcations and chaotic dynamics. Up to now, few researchers have made of the energy-phase method to study the Shilnikov-type multi-pulse homoclinic and heteroclinic bifurcations and chaotic dynamics of high-dimensional nonlinear systems in engineering applications. Malhotra et al. [29] used the energy-phase method to investigate multi-pulse homoclinic orbits and chaotic dynamics for the motion of flexible spinning discs. In papers [30–32], Zhang and Yao utilized the energy-phase method to analyze the Shilnikov-type multi-pulse homoclinic or heteroclinic orbits and chaotic dynamics in some engineering problems, for example, in the nonlinear non-planar oscillations of the cantilever beam, in a parametrically excited viscoelastic moving belt, and in a parametrically and externally excited rectangular thin plate.

In addition, De Feo [33,34] numerically and theoretically investigated the qualitative resonance phenomenon of the multi-pulse Shilnikov-like strange attractors for two classes of three-dimensional nonlinear systems.

Early researches on the nonlinear non-planar oscillations of cantilever beams focused on establishing the model and analyzing nonlinear responses of cantilever beams. Crespo da Silva and Glynn [35,36] formulated a set of integral-partial differential governing equations of motion describing the nonlinear non-planar oscillations of an inextensional cantilever beam and utilized the method of multiple scales to study forced resonant oscillations of the cantilever beam. Crespo da Silva and Glynn [37] investigated the nonlinear non-planar, flexural–torsional oscillations of a clamped–clamped/sliding beam under a planar distributed harmonic excitation. In another paper [38], the nonlinear non-planar oscillations and response of a cantilever beam with asymmetric support conditions were studied by Crespo da Silva and Glynn. Zaretzky and Crespo da Silva [39] gave an experimental investigation for the nonlinear non-planar motion of cantilever beams excited by a periodic transverse base excitation.

Recent research works on the nonlinear non-planar oscillations of cantilever beams focus on analyzing complex nonlinear dynamics and controlling chaos and oscillations of cantilever beams. Nayfeh and Pai [40] used the Galerkin procedure and the method of multiple scales to investigate the nonlinear planar and non-planar responses of the inextensional cantilever beams and found that the nonlinear geometric

terms produce a hardening effect and dominate the non-planar responses for all modes. The non-planar responses of a cantilevered beam subjected to lateral harmonic base-excitation were also analyzed by Pai and Nayfeh [41] using two nonlinear coupled integro-differential equations of motion. Cusumano and Moon [42,43] presented the results for an externally excited thin elastica. Anderson et al. [44] analytically and experimentally investigated the response of the cantilever beam with widely separated natural frequencies and observed that the response consisted of the first, third, and fourth modes. Arafat et al. [45] studied the nonlinear non-planar response of the cantilever inextensional metallic beams to a principal parametric excitation and found that there exist the bifurcations and chaotic motion. Esmailzadeh and Nakhaie-Jazar [46] investigated the nonlinear parametric vibration of a massless cantilever beam with a lumped mass attached to its free end while being excited harmonically at the base. Hamdan et al. [47] analyzed the second-order approximations of the nonlinear planar responses and the steady-state principal parametric resonance response of a vertically mounted flexible cantilever beam subjected to a vertical harmonic base motion.

Recently, Siddiqui et al. [48] analyzed large amplitude motion of a cantilever beam carrying a moving spring–mass and obtained the nonlinear responses. Malatkar and Nayfeh [49] gave an experimental and theoretical study of the nonlinear response of a flexible cantilever beam to an external harmonic excitation and demonstrated the energy transfer from the third mode to the first mode. Dwivedy and Kar [50] used the method of multiple scales to study the periodic, quasi-periodic and chaotic responses of a parametrically excited cantilever beam with an attached mass. Young and Juan [51] studied the nonlinear response of a fluttered, cantilevered beam subjected to a random follower force at the free end. In 2005, Zhang and Yao [30] utilized the energy-phase method to analyze the Shilnikov-type multi-pulse homoclinic and heteroclinic orbits and chaotic dynamics in the nonlinear non-planar oscillations of the cantilever beam. Zhang [52] investigated the chaotic motion and its control for the nonlinear non-planar oscillations of a parametrically excited cantilever beam.

The studies of this paper focus on the multi-pulse homoclinic orbits and chaotic dynamics for the nonlinear non-planar oscillations of a cantilever beam which is subjected to a harmonic axial excitation and two transverse excitations at the free end. The extended Melnikov method for studying the Shilnikov-type multi-pulse homoclinic orbits in high-dimensional nonlinear systems is briefly demonstrated in the theoretical frame. The nonlinear governing equations of non-planar motion for the cantilever beam are obtained. The Galerkin procedure is applied to the partial differential governing equations to obtain a two-degree-of-freedom nonlinear system under combined parametric and forcing excitations. The principal parametric resonance–1/2 subharmonic resonance for the in-plane mode and fundamental parametric resonance–primary resonance for the out-of-plane mode are considered. The method of multiple scales is utilized to transform the parametrically and externally excited two-degree-of-freedom nonlinear system to the autonomous averaged equation. Based on the averaged equation, the theory of normal form is used to find the explicit formulas of normal form. The extended Melnikov method presented by Camassa et al. [22] is employed to analyze the multi-pulse homoclinic orbits and chaotic dynamics for the nonlinear non-planar oscillations of the cantilever beam. The analysis indicates that there exists the multi-pulse jumping of the heteroclinic orbits for the averaged equation. The results of numerical simulation also show that the Shilnikov-type multi-pulse chaotic motions can occur for the nonlinear non-planar oscillations of the cantilever beam, which verifies the analytical prediction.

2. The extended Melnikov method

The extended Melnikov method was first presented by Camassa et al. in 1998 [22], which is an extension of the global perturbation method developed by Kovacic and Wiggins [4]. It is different from the global perturbation technique developed by Kovacic and Wiggins [4]. This method can be utilized to detect the Shilnikov-type multi-pulse homoclinic or heteroclinic orbits and chaotic dynamics to slow manifolds of near-integrable four-dimensional or higher-dimensional nonlinear systems. In this section, we will give a briefly description on the extended Melnikov method based on the paper given by Camassa et al. [22].

2.1. The extended Melnikov method for homoclinic orbits

The system considered here is of the form

$$\dot{x} = JD_x H(x, I) + \varepsilon g^x(x, I, \gamma, \mu, \varepsilon), \tag{2.1a}$$

$$\dot{I} = \varepsilon g^I(x, I, \gamma, \mu, \varepsilon), \tag{2.1b}$$

$$\dot{\gamma} = \Omega(x, I) + \varepsilon g^\gamma(x, I, \gamma, \mu, \varepsilon), \tag{2.1c}$$

where $x = (x_1, x_2) \in \mathbf{R}^2$, $I \in \mathbf{R}$, $\gamma \in \mathbf{S}^1$, $\mathbf{P} = \mathbf{R}^2 \times \mathbf{R} \times \mathbf{S}^1$, $H(x, I)$ is a Hamiltonian function with respect to the variables x and I, $\mu \in \mathbf{R}$ is a real parameter, $\varepsilon \ll 1$ is a small parameter. In addition, D_x and D_I, respectively, represent the partial derivatives with respect to x and I.

The matrix J given in Eq. (2.1) is of the form

$$J = \begin{pmatrix} 0 & 1 \\ -1 & 0 \end{pmatrix}. \tag{2.2}$$

Let $\langle \cdot, \cdot \rangle$ denote the usually Euclidean inner product in $\mathbf{R}^n$, where n is the dimension of the vectors in the arguments, and denote by $\|\cdot\|$ the induced Euclidean norm, as well as the corresponding matrix norm.

Setting $\varepsilon = 0$ in Eq. (2.1) leads to the unperturbed system

$$\dot{x} = JD_x H(x, I), \tag{2.3a}$$

$$\dot{I} = 0, \tag{2.3b}$$

$$\dot{\gamma} = \Omega(x, I). \tag{2.3c}$$

It is observed from the aforementioned analysis that Eq. (2.3a) is a Hamiltonian system which is independent of the variable γ. We now make two assumptions given by Camassa et al. [22] for the unperturbed Eq. (2.3). The first assumption concerns the smoothness of the functions in Eq. (2.3).

Assumption 2.1. The unperturbed Hamiltonian $H(x, I)$ is a real-analytic function of its arguments.

The second assumption introduces the presence of the homoclinic orbits in the phase space of Eq. (2.3).

Assumption 2.2. For every I with $I_1 < I < I_2$, Eq. (2.3a) possesses a hyperbolic singular point $x = \bar{x}_0(I)$, which varies continuously with I, and whose stable and unstable manifolds, $W^s(\bar{x}_0(I))$ and $W^u(\bar{x}_0(I))$, intersect along a homoclinic orbit $W(\bar{x}_0(I))$ connecting the singular point at $x = \bar{x}_0(I)$ to itself.

Because of the hyperbolicity of the singular point $x = \bar{x}_0(I)$, the Jacobi matrix $JD_x^2 H(\bar{x}_0(I), I)$ must have a pair of non-zero real eigenvalues. Moreover, the implicit function theorem for the analytic functions immediately implies that the vector $\bar{x}_0(I)$ analytically depends on the variable I. Since Eq. (2.3a) is an autonomous system, all the solutions on the homoclinic orbit $W(\bar{x}_0(I))$ have a representation of the form $x^h(t - t_0, I)$. Setting $t_0 = 0$ and varying t in the solution $x^h(t - t_0, I)$, we can obtain a consistent parametrization of individual orbits in the manifold $W(\bar{x}_0(I))$.

In full four-dimensional (x, I, γ) phase space of system (2.3), each singular point $\bar{x}_0(I)$ corresponds to a periodic orbit O^I parametrized by the solution

$$O^I = \left\{ (x, I, \gamma) \,\middle|\, x = \bar{x}_0, I, \Omega(\bar{x}_0(I), I)t + \gamma_0 \right\}. \tag{2.4}$$

Each of these periodic orbits possesses two-dimensional stable and unstable manifolds, $W^s(O^I)$ and $W^u(O^I)$, which are the Cartesian products of the stable and unstable manifolds $W^s(\bar{x}_0(I))$ and $W^u(\bar{x}_0(I))$ of the singular point $\bar{x}_0(I)$ and the phase angle γ. The existence of the homoclinic manifolds $W(\bar{x}_0(I))$ implies that the manifolds $W^s(O^I)$ and $W^u(O^I)$ coincide along a two-dimensional homoclinic manifold $W(O^I)$.

A two-dimensional invariant annulus, which is denoted by M, can be obtained by taking the set of the orbits O^I over all $I_1 < I < I_2$. The annulus M possesses three-dimensional stable and unstable manifolds, $W^s(M)$ and $W^u(M)$, which intersect along three-dimensional homoclinic manifold $W(M)$. All these manifolds are the unions of the manifolds $W^s(O^I)$, $W^u(O^I)$, and $W(O^I)$ along the interval $I_1 < I < I_2$. The homoclinic manifold

$W(M)$ is parametrized by t, I and γ_0 in the solutions

$$x = x^h(t,I), \quad I = I, \quad \gamma = \gamma^h(t,I) + \gamma_0 = \int_0^t \Omega(x^h(\tau,I),I)\,\mathrm{d}\tau + \gamma_0. \tag{2.5}$$

The aforementioned solutions are also rewritten as

$$X_0(t,I,\gamma_0) = \left(x^h(t,I), I_1 < I < I_2, \int_0^t \Omega(x^h(\tau,I),I)\,\mathrm{d}\tau + \gamma_0 \right). \tag{2.6}$$

The homoclinic manifolds $W(M)$ can be obtained by solving the equation

$$H(x,I) - H(\bar{x}_0(I),I) = 0. \tag{2.7}$$

The phase shift or phase jump of system (2.3) can be also calculated as

$$\Delta\gamma(I) = \int_{-\infty}^{+\infty} \left[\Omega(x^h(\tau,I),I) - \Omega(\bar{x}_0(I),I) \right]\mathrm{d}\tau. \tag{2.8}$$

The aforementioned results of the hyperbolic structure persist for sufficiently small $\varepsilon > 0$. In particular, persistence results indicate that the unperturbed annulus M persists together with its local stable and unstable manifolds, $W_{\mathrm{loc}}^s(M)$ and $W_{\mathrm{loc}}^u(M)$, that is, the connected pieces of the stable and unstable manifolds $W^s(M)$ and $W^u(M)$ are contained in some small enough neighborhood of M and intersect along M. This ensures the existence of an $O(\varepsilon)$ close, non-unique, locally invariant annulus M_ε and its local stable and unstable manifolds $W_{\mathrm{loc}}^s(M_\varepsilon)$ and $W_{\mathrm{loc}}^u(M_\varepsilon)$, which are $O(\varepsilon)$ close to local manifolds $W_{\mathrm{loc}}^s(M)$ and $W_{\mathrm{loc}}^u(M)$. The tangent spaces of two manifolds are also $O(\varepsilon)$-close. Local invariance of the annulus M_ε reflects the fact which M_ε may leak phase points through its boundary, and is also responsible for the non-uniqueness of M_ε. This non-uniqueness does not present any major difficulties, since all the copies of the annulus M_ε must contain all the invariant sets which are contained in any one of them.

In the following, several definitions will be given. First, we define the Melnikov function, $M(I, \gamma_0, \mu)$, which is given by the integral:

$$M(I,\gamma_0,\mu) = \int_{-\infty}^{+\infty} \left\langle \mathbf{n}(p^h(t)), \mathbf{g}(p^h(t),\mu,0) \right\rangle \mathrm{d}t, \tag{2.9}$$

where the vector $\mathbf{n}$ is the normal to the homoclinic manifold $W(M)$, and

$$\mathbf{n} = (D_x H(x,I), D_I H(x,I) - D_I H(\bar{x}_0(I),I), 0), \tag{2.10}$$

$$\mathbf{g} = (g^x(x,I,\gamma,\mu,0), g^I(x,I,\gamma,\mu,0), g^\gamma(x,I,\gamma,\mu,0)), \tag{2.11}$$

and

$$p^h(t) = (x^h(t,I), I, \gamma^h(t,I) + \gamma_0) \tag{2.12}$$

is any homoclinic orbit (2.5) of unperturbed system (2.3).

Second, we define the signature σ of the normal $\mathbf{n}$ to the unperturbed homoclinic manifold $W(M)$ by the formula

$$\sigma = \lim_{t\to+\infty} \frac{\left\langle n(P^h(t)), \dot{P}^h(-t) \right\rangle}{\left\| D_x H(x^h(t,I),I) \right\| \left\| D_x H(x^h(-t,I),I) \right\|} = \lim_{t\to+\infty} \frac{\left\langle D_x H(x^h(t,I),I), J D_x H(x^h(-t,I),I) \right\rangle}{\left\| D_x H(x^h(t,I),I) \right\| \left\| D_x H(x^h(-t,I),I) \right\|}. \tag{2.13}$$

Therefore, the signature σ is positive if the normal $\mathbf{n}$ to the unperturbed homoclinic manifold $W(M)$ points in the direction of the unperturbed flow on the unstable manifold $W^u(M)$ at a point $(\bar{x}_0(I), I, \gamma)$ in the annulus M, and negative otherwise. It is noticed that $\sigma \neq 0$ due to the transversality of the intersection between the manifolds $W^s(\bar{x}_0(I))$ and $W^u(\bar{x}_0(I))$ at the equilibria $\bar{x}_0(I)$.

Third, we also need to define the k-pulse Melnikov function $M_k(\varepsilon, I, \gamma_0, \mu)$, $(k = 1,2,\ldots)$ as

$$M_k(\varepsilon,I,\gamma_0,\mu) = \sum_{j=0}^{k-1} M(I, j\Delta\gamma(I) + \Gamma_j(\varepsilon,I,\gamma_0,\mu) + \gamma_0, \mu), \tag{2.14}$$

where

$$\Gamma_j(\varepsilon, I, \gamma_0, \mu) = \frac{\Omega(\bar{x}_0(I), I)}{\lambda(I)} \sum_{r=1}^{j} \log \left| \frac{\zeta(I)}{\varepsilon M_r(\varepsilon, I, \gamma_0, \mu)} \right| \tag{2.15}$$

for $j = 1, \ldots, k-1$ and $\Gamma_0(\varepsilon, I, \gamma_0, \mu) = 0$. Thus, the 1-pulse Melnikov function $M_1(\varepsilon, I, \gamma_0, \mu)$ coincides with the standard Melnikov function $M(I, \gamma_0, \mu)$ given by Eq. (2.9). The function $\varsigma(I)$ is defined by the Jacobi matrix of Eq. (2.3a) at the singular point $x = \bar{x}_0(I)$ as

$$\zeta(I) = \frac{2(\lambda(I))^2 |A_2(I)| f_+(I) f_-(I)}{\sqrt{[(A_2(I))^2 + (\lambda(I) - A_0(I))^2][(A_2(I))^2 + (\lambda(I) + A_0(I))^2]}}, \tag{2.16}$$

where

$$A_0(I) = D_{x_1} D_{x_2} H(\bar{x}_0(I), I), A_1(I) = D_{x_1}^2 H(\bar{x}_0(I), I), A_2(I) = D_{x_2}^2 H(\bar{x}_0(I), I),$$

$$f_+(I) = \lim_{t \to +\infty} \frac{1}{\lambda(I)} e^{\lambda(I)t} \| D_x H(x^h(t, I), I) \|, \quad f_-(I) = \lim_{t \to -\infty} \frac{1}{\lambda(I)} e^{-\lambda(I)t} \| D_x H(x^h(t, I), I) \|. \tag{2.17}$$

It is noticed that if for some I the frequency $\omega(I) = \Omega(\bar{x}_0(I), I)$ equals to zero, that is, if the periodic orbit corresponding to this I value degenerates into a circle of equilibria, the contribution from the functions $\Gamma_j(\varepsilon, I, \gamma_0, \mu)$ vanishes identically in the k-pulse Melnikov function $M_k(\varepsilon, I, \gamma_0, \mu)$.

The main results are given as follows.

Theorem 2.1. *For some integer* k, *some constant* $B > 0$ *independent of* ε, *some* $I = \bar{I}$, *some* $\mu = \bar{\mu}$, *and all sufficiently small* $\varepsilon > 0$, *let there exist a function* $\gamma_0 = \bar{\gamma}_0(\varepsilon)$, *such that the following conditions are satisfied:*

(1) *The* k-*pulse Melnikov function has a simple zero in* γ_0, *namely,* $M_k(\varepsilon, \bar{I}, \bar{\gamma}_0(\varepsilon), \bar{\mu}) = 0$, *and* $\left| D_{\gamma_0} M_k(\varepsilon, \bar{I}, \bar{\gamma}_0(\varepsilon), \bar{\mu}) \right| > B$.
(2) $M_i(\varepsilon, \bar{I}, \bar{\gamma}_0(\varepsilon), \bar{\mu}) \neq 0$ *for all* $i = 1, \ldots, k-1$, $k > 1$, *and is positive if the signature* σ *of the normal* $\mathbf{n}$ *is positive, and negative if* σ *is negative.*
(3) *For all* $i = 1, \ldots, k-1$, $k > 1$,

$$\left| \frac{1 - [\Omega(\bar{x}_0(\bar{I}), \bar{I})/\lambda(\bar{I})] D_{\gamma_0} \log |M_1 M_2 \ldots M_i| (\varepsilon, \bar{I}, \bar{\gamma}_0(\varepsilon), \bar{\mu})}{1 - [\Omega(\bar{x}_0(\bar{I}), \bar{I})/\lambda(\bar{I})] D_{\gamma_0} \log |M_1 M_2 \ldots M_{i-1}| (\varepsilon, \bar{I}, \bar{\gamma}_0(\varepsilon), \bar{\mu})} \right| > B, \tag{2.18}$$

where the denominator in Eq. (2.18) is defined to be 1 when $i = 1$.

Then, for all I close to $\bar{I}$, all μ close to $\bar{\mu}$, and all sufficiently small ε, there exists a two-dimensional intersection surface $\sum_{\varepsilon}^{\mu}(\bar{\gamma}_0)$ along which the stable and unstable manifolds $W^s(M_\varepsilon)$ and $W^u(M_\varepsilon)$ of the annulus M_ε intersect transversely at a phase angle of size $O(\varepsilon)$. Moreover, outside of a small neighborhood of the annulus M_ε, the surface $\sum_{\varepsilon}^{\mu}(\bar{\gamma}_0)$ is $O(\varepsilon)$-close to the surface spanned by the set of the orbits in Eq. (2.6) selected by the phase angles

$$\gamma_0 = \hat{\gamma}_0(\varepsilon, I, \mu) + j\Delta\gamma(I) + \Gamma_j(\varepsilon, I, \hat{\gamma}_0(\varepsilon, I, \mu), \mu), \quad j = 0, \ldots, k-1, \tag{2.19}$$

where the triple $(I, \hat{\gamma}_0(\varepsilon, I, \mu), \mu)$ identically satisfies the following equation:

$$M_k(\varepsilon, I, \hat{\gamma}_0(\varepsilon, I, \mu), \mu) = 0$$

in some neighborhood of $I = \bar{I}$ and $\mu = \bar{\mu}$, and $\hat{\gamma}_0(\varepsilon, \bar{I}, \bar{\mu}) = \bar{\gamma}_0(\varepsilon)$.

The extended Melnikov function is computed by a recursion procedure from the usual one-pulse Melnikov function, and depends on the small perturbation parameter ε, which is at variance with the usual Melnikov method and is particular to the general case of slow dynamics on the hyperbolic manifold. Moreover, the dependence on ε is through a logarithmic function, which makes the calculation of the asymptotics in the small ε limit particularly delicate.

In the following analysis, we will apply Theorem 2.1 to a resonance case. In this case, the computation of the k-pulse Melnikov function will be reduced. We also make the following assumption.

Assumption 2.3. For some $I = I_r \in (I_1, I_2)$, the frequency $\omega(I) = \Omega(\bar{x}_0(I), I)$ pass through a simple zero at the I_r, that is

$$\omega(I_r) = \Omega(\bar{x}_0(I_r), I_r) = 0, \quad D_I \omega(I_r) \neq 0. \tag{2.20}$$

Then, it is known from Eq. (2.20) that a resonance occurs for $I = I_r$, which is referred to as a resonant I value. The singular points corresponding to I_r are also referred to as resonant singular points.

To focus on a neighborhood of the resonant value $I = I_r$, the following transformation is introduced:

$$I = I_r + \sqrt{\varepsilon}h, \quad h \in [-h_0, h_0], \quad \gamma = \gamma, \tag{2.21}$$

where $h_0 > 0$ will be determined later.

Transformation (2.21) blows up the resonance band

$$P_{\sqrt{\varepsilon}} = \left\{ (x, I, \gamma) \in \mathbf{P} \, \middle| \, I \in \left[I_r - h_0\sqrt{\varepsilon}, I_r + h_0\sqrt{\varepsilon} \right] \right\} \tag{2.22}$$

of the phase space $\mathbf{P}$. We will be interested in finding the trajectories of Eq. (2.1) for $\varepsilon > 0$ which are doubly asymptotic to the near-resonance band $M_\varepsilon^R = M_\varepsilon \cap P_{\sqrt{\varepsilon}}$ of the invariant manifold M_ε.

Substituting the transformation (2.21) into the later two equations of Eq. (2.1) and making a simple Taylor expansion in powers of $\sqrt{\varepsilon}$, we obtain the following equation:

$$h' = g^I(\bar{x}_0(I_r), I_r, \gamma, \mu) + \sqrt{\varepsilon}G(h, \gamma, \mu) + O(\varepsilon), \tag{2.23a}$$

$$\gamma' = \frac{\mathrm{d}}{\mathrm{d}I}[\Omega(\bar{x}_0(I_r), I_r)]h + \sqrt{\varepsilon}F(h, \gamma, \mu) + O(\varepsilon), \tag{2.23b}$$

where the prime represents the differentiation with respect to $\sqrt{\varepsilon}t$, and

$$G(h, \gamma, \mu) = \frac{\mathrm{d}}{\mathrm{d}I}\left[g^I(\bar{x}_0(I_r), I_r, \gamma, \mu) \right]h, \tag{2.24}$$

$$F(h, \gamma, \mu) = \frac{1}{2}\frac{\mathrm{d}^2}{\mathrm{d}I^2}[\Omega(\bar{x}_0(I_r), I_r)]h^2 + D_x\Omega(\bar{x}_0(I_r), I_r)\bar{x}_1(I_r, \gamma, \mu) + g^\gamma(\bar{x}_0(I_r), I_r, \gamma, \mu), \tag{2.25}$$

where $\bar{x}_1(I_r, \gamma, \mu)$ is given as follows:

$$\bar{x}_1 = \left[JD_x^2 H(\bar{x}_0(I_r), I_r) \right]^{-1} \left(g^I(\bar{x}_0(I_r), I_r, \gamma, \mu)D_I\bar{x}_0(I_r) - g^x(\bar{x}_0(I_r), I_r, \gamma, \mu) \right). \tag{2.26}$$

We can use Theorem 2.1 in the original (x, I, γ) coordinates to determine the existence of a possible surviving k-pulse homoclinic intersection surface $\sum_\varepsilon^\mu(\bar{\gamma}_0)$. It is noticed that in this case, for any integer k, the k-pulse Melnikov function at the resonance $I = I_r$ is given as follows:

$$M_k(I_r, \gamma_0, \mu) = \sum_{j=0}^{k-1} M(I_r, \gamma_0 + j\Delta\gamma(I_r), \mu), \tag{2.27}$$

where the Melnikov function $M(I_r, \gamma_0, \mu)$ is given by Eq. (2.9) with $I = I_r$, and the phase shift is given based on Eq. (2.8)

$$\Delta\gamma(I_r) = \int_{-\infty}^{+\infty} \Omega(x^h(\tau, I_r), I_r)\,\mathrm{d}\tau. \tag{2.28}$$

At the resonance value I_r, there is $\Omega(\bar{x}_0(I_r), I_r) = 0$. Therefore, it is noticed that the k-pulse Melnikov function (2.27) in the resonance case of the orbits homoclinic to resonance band does not depend on ε, and $\Gamma_j(\varepsilon, I_r, \gamma_0, \mu) = 0$ $(j = 0, 1, \ldots, k-1)$. In many engineering applications, in general, only resonant cases are considered to demonstrate main nonlinear behaviors in engineering systems. Therefore, in the resonant case, we can simplify the computing procedure of the extended Melnikov function because of $\Gamma_j(\varepsilon, I_r, \gamma_0, \mu) = 0$

($j = 0,1,\dots,k-1$). In the resonance case of the orbits homoclinic to resonance band, Theorem 2.1 becomes the following proposition.

Proposition 2.3. *In the resonance case $I = I_r$, for some integer k and $\mu = \bar{\mu}$, let there exist a phase angle $\gamma_0 = \bar{\gamma}_0$, such that the following conditions are satisfied*:

(1) *The k-pulse Melnikov function has a simple zero in γ_0, that is*

$$M_k(I_r, \bar{\gamma}_0, \bar{\mu}) = 0, \quad D_{\gamma_0} M_k(I_r, \bar{\gamma}_0, \bar{\mu}) \neq 0. \tag{2.29}$$

(2) $M_i(I_r, \bar{\gamma}_0, \bar{\mu}) \neq 0$ *for all $i = 1,\dots,k-1$, $k > 1$, and is positive if the signature σ of the normal $\mathbf{n}$ is positive, and negative if the signature σ is negative.*

Then, for all I close to I_r, all μ close to $\bar{\mu}$, there exists a two-dimensional intersection surface $\sum_{\varepsilon}^{m}(\bar{\gamma}_0)$ along which the stable and unstable manifolds $W^s(M_\varepsilon)$ and $W^u(M_\varepsilon)$ of the annulus M_ε intersect transversely at a phase angle of size $O(\varepsilon)$. In the (x, h, γ) variables, outside of a small neighborhood of the annulus M_ε, the surface $\sum_{\varepsilon}^{\mu}(\bar{\gamma}_0)$ collapses smoothly onto the union of the surface $\sum_{\varepsilon}^{\mu}(\bar{\gamma}_0)$ spanned by the set of the orbits parametrized by Eq. (2.6) with $\gamma_0 = \bar{\gamma}_0(\mu) + j\Delta\gamma(I_r)$, $j = 0,\dots,k-1$, and with arbitrary h. Here $\bar{\gamma}_0(\mu)$ is the corresponding simple zero of the k-pulse Melnikov function $M_k(I_r, \gamma_0, \mu)$. The surface $\sum_{\varepsilon}^{\mu}(\bar{\gamma}_0)$ takes off from the cylinder M_0 along the line $\gamma = \gamma_0(\mu) - \Delta\gamma^-(I_r)$ and eventually lands back on it along the line $\gamma = \bar{\gamma}_0(\mu) + (k-1)\Delta\gamma(I_r) + \Delta\gamma^+(I_r)$, where the phase differences $\Delta\gamma^-(I_0)$ and $\Delta\gamma^+(I_0)$ are defined as

$$\Delta\gamma^+(I_0) = \int_0^{+\infty} \Omega(x^h(\tau, I_r), I_r)\,\mathrm{d}\tau, \quad \Delta\gamma^-(I_r) = \int_{-\infty}^0 \Omega(x^h(\tau, I_r), I_r)\,\mathrm{d}\tau. \tag{2.30}$$

Recall that the signature σ does not need to be computed if the region enclosed by the unperturbed homoclinic manifold $W(M_\varepsilon)$ is convex. We refer to the limiting surface $\sum_{\varepsilon}^{\mu}(\bar{\gamma}_0)$ as a singular homoclinic intersection surface.

In Section 5, we will give the application of the extended Melnikov method to the nonlinear non-planar oscillations of the cantilever beam subjected to a harmonic axial excitation and two transverse excitations at the free end.

3. Equations of non-planar motion for a cantilever beam

We consider a cantilever beam with length L, mass m per unit length and subjected to a harmonic axial excitation and two transverse excitations at the free end, as shown in Fig. 1(a). Assume that the beam considered here is an Euler–Bernoulli beam. A Cartesian coordinate system, $Oxyz$, is adopted, which is located in the symmetric plane of the cantilever beam. The s denotes the curve coordinate along the elastic axis before the deformation. The ξ, η and ς are the principal axes of the cross section for the cantilever beam at position s, as shown in Fig. 1(b). The symbols $v(s, t)$ and $w(s, t)$ denote the displacements of a point in the middle line of the cantilever beam in the y and z directions, respectively. For later convenience, the harmonic axial excitation may be expressed in the form $2F_1 \cos \Omega_1 t$. The transverse excitations in the y and z directions are represented in the forms $2F_2 \cos \Omega_2 t$ and $2F_3(s)\cos \Omega_2 t$, respectively. The non-dimensional nonlinear governing equations of non-planar motion for the cantilever beam under combined parametric and forcing excitations are of the following form [18]:

$$\ddot{v} + \bar{c}\dot{v} + \beta_y v^{iv} + F_1 \cos(\Omega_1 t)v'' = (1 - \beta_y)\left[w'' \int_1^s v''w'' \,\mathrm{d}s - w''' \int_0^s v''w' \,\mathrm{d}s\right]' - \frac{1}{\beta_\gamma}(1 - \beta_y)^2 \left[w'' \int_0^s \int_1^s v''w'' \,\mathrm{d}s\,\mathrm{d}s\right]''$$

$$- \beta_y[v'(v'v'' + w'w'')']' - \frac{1}{2}\left[v' \int_1^s \frac{\mathrm{d}^2}{\mathrm{d}t^2}\left\{\int_0^s \left(v'^2 + w'^2\right)\mathrm{d}s\right\}\mathrm{d}s\right]'$$

$$- F_1 \cos(\Omega_1 t)\left[v'\left(v'^2 + w'^2\right)\right]' + F_2(s)\cos(\Omega_2 t), \tag{3.1a}$$
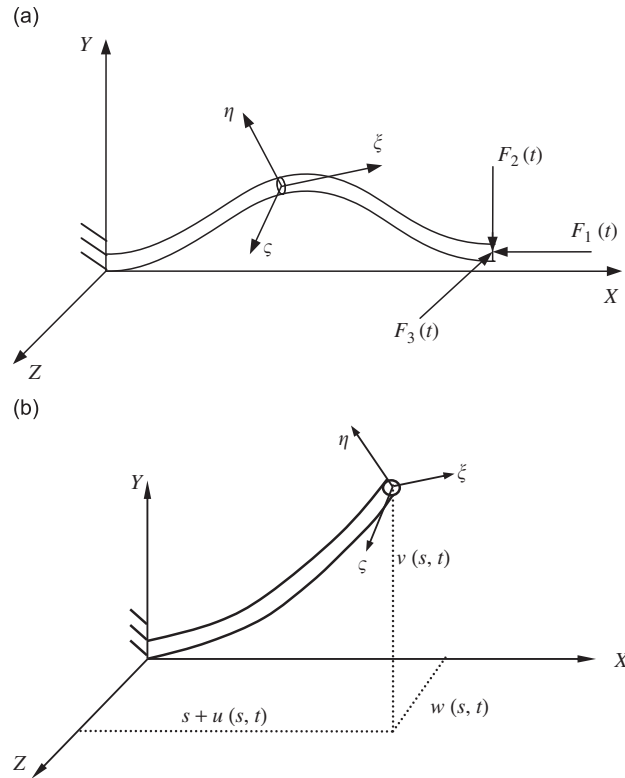
Fig. 1. The model of a cantilever beam with length L, mass m per unit length and subjected to a harmonic axial excitation and transverse excitations at the free end: (a) the model and (b) a segment.

$$
\ddot{w} + \bar{c}\dot{w} + w^{iv} + F_1 \cos(\Omega_1 t)w'' = -(1 - \beta_y)\left[v'' \int_1^s v''w'' \, ds - v''' \int_0^s w''v' \, ds \right]'
$$
$$
- \frac{1}{\beta_\gamma}(1 - \beta_y)^2 \left[v'' \int_0^s \int_1^s v''w'' \, ds \, ds \right]'' - [w'(v'v'' + w'w'')']'
$$
$$
- \frac{1}{2}\left[w' \int_1^s \frac{d^2}{dt^2}\left\{ \int_0^s \left(v'^2 + w'^2 \right) ds \right\} ds \right]' - F_1 \cos(\Omega_1 t)\left[w'\left(v'^2 + w'^2 \right) \right]'
$$
$$
+ F_3(s)\cos(\Omega_2 t), \tag{3.1b}
$$

where the dots and primes, respectively, represent partial differentiation with respect to t and x, the $\bar{c}$ is the damping coefficient, and the β_y is the ratio between the in-plane and out-of-plane principal flexural stiffnesses, that is, $\beta_y = D_\zeta / D_\eta$.

The boundary conditions are represented as

$$
v(0, t) = w(0, t) = v'(0, t) = w'(0, t) = 0, \tag{3.2a}
$$

$$
v''(1, t) = w''(1, t) = v'''(1, t) = w'''(1, t) = 0. \tag{3.2b}
$$

In the following analysis, we apply the Galerkin procedure to Eq. (3.1) to obtain a two-degree-of-freedom nonlinear system under combined parametric and forcing excitations. The planar and non-planar flexural modes for the cantilever beam are considered as

$$
v(s, t) = y(t)G(s), \quad w(s, t) = z(t)G(s), \tag{3.3}
$$

where the function $G(s)$ is a linear mode of the transverse free vibration for the cantilever beam and is of the following form:

$$G(s) = \cosh(rs) - \cos(rs) - \left[(\cosh(r) + \cos(r))/(\sinh(r) + \sin(r))\right][\sinh(rs) - \sin(rs)]. \tag{3.4}$$

Introduce the time variable $\hat{t} = r^2 t$. For convenience of the following analysis, we drop the hat. Substituting Eq. (3.3) into Eq. (3.1), multiplying Eq. (3.1) by $G(s)$ and integrating to s from 0 to 1, a two-degree-of-freedom nonlinear system under combined parametric and forcing excitations is obtained as

$$\ddot{y} + c\dot{y} + \beta_y y - 2\alpha_1 F_1 \cos(\Omega_1 t)y + \alpha_2 y(y\ddot{y} + \dot{y}^2 + z\ddot{z} + \dot{z}^2) + \alpha_3 \beta_y y^3$$
$$+ \left[\beta_y \alpha_3 + (1 - \beta_y)\alpha_4 - \frac{1}{\beta_y}(1 - \beta_y)^2 \alpha_5\right] yz^2 - 2\bar{F}_1 \cos(\Omega_1 t)(y^3 + yz^2) = f_1 \cos \Omega_2 t, \tag{3.5a}$$

$$\ddot{z} + c\dot{z} + z - 2\alpha_1 F_1 \cos(\Omega_1 t)z + \alpha_2 z(y\ddot{y} + \dot{y}^2 + z\ddot{z} + \dot{z}^2) + \alpha_3 z^3$$
$$- \left[(1 - \beta_y)\alpha_4 + \frac{1}{\beta_y}(1 - \beta_y)^2 \alpha_5 - \beta_y \alpha_3\right] zy^2 - 2\bar{F}_1 \cos(\Omega_1 t)(z^3 + zy^2) = f_2 \cos \Omega_2 t, \tag{3.5b}$$

where the dots denote partial differentiation with respect to $\hat{t}$, and

$$\alpha_1 = -\frac{1}{r^4}\int_0^1 GG''\,ds, \quad \alpha_2 = \int_0^1 G\left[G'\int_1^s\int_0^s G'^2\,ds\,ds\right]'ds, \quad \alpha_3 = \frac{1}{r^4}\int_0^1 G\left[G'(G'G'')'\right]'ds$$

$$\alpha_4 = -\frac{1}{r^4}\int_0^1 G\left[G''\int_1^s G''^2\,ds - G'''\int_0^s G'G''\,ds\right]'ds, \quad \alpha_5 = -\frac{1}{r^4}\int_0^1 G\left[G''\int_0^s\int_1^s G''^2\,ds\,ds\right]''ds$$

$$c = \frac{\bar{c}}{r^2}, \quad \bar{F}_1 = -\frac{F_1}{2r^4}\int_0^1 G\left(G'^3\right)'ds, \quad f_1 = \frac{1}{r^4}\int_0^1 GF_2\,ds, \quad f_2 = \frac{1}{r^4}\int_0^1 GF_3\,ds. \tag{3.6}$$

To obtain a system which is suitable for the application of the method of multiple scales [53], the scale transformations may be introduced as

$$\alpha_2 \to \varepsilon\alpha_2, \quad \alpha_3 \to \varepsilon\alpha_3, \quad \alpha_4 \to \varepsilon\alpha_4, \quad \alpha_5 \to \varepsilon\alpha_5,$$
$$F_1 \to \varepsilon F_1, \quad \bar{F}_1 \to \varepsilon^2 \bar{F}_1, \quad c \to \varepsilon c, \quad f_1 \to \varepsilon f_1, \quad f_2 \to \varepsilon f_2, \tag{3.7}$$

where ε is a small perturbation parameter.

Substituting Eq. (3.7) into Eq. (3.5), we obtain the following dimensionless two-degree-of-freedom nonlinear system:

$$\ddot{y} + \varepsilon c\dot{y} + \beta_y y - 2\varepsilon\alpha_1 F_1 \cos(\Omega_1 t)y + \varepsilon\alpha_2 y(y\ddot{y} + \dot{y}^2 + z\ddot{z} + \dot{z}^2) + \varepsilon\alpha_3 \beta_y y^3$$
$$+ \varepsilon\left[\beta_y\alpha_3 + (1 - \beta_y)\alpha_4 - \frac{1}{\beta_y}(1 - \beta_y)^2\alpha_5\right] yz^2 - 2\varepsilon^2\bar{F}_1 \cos(\Omega_1 t)(y^3 + yz^2) = \varepsilon f_1 \cos \Omega_2 t, \tag{3.8a}$$

$$\ddot{z} + \varepsilon c\dot{z} + z - 2\varepsilon\alpha_1 F_1 \cos(\Omega_1 t)z + \varepsilon\alpha_2 z(y\ddot{y} + \dot{y}^2 + z\ddot{z} + \dot{z}^2) + \varepsilon\alpha_3 z^3$$
$$+ \varepsilon\left[\beta_y\alpha_3 - (1 - \beta_y)\alpha_4 - \frac{1}{\beta_y}(1 - \beta_y)^2\alpha_5\right] zy^2 - 2\varepsilon^2\bar{F}_1 \cos(\Omega_1 t)(z^3 + zy^2) = \varepsilon f_2 \cos \Omega_2 t, \tag{3.8b}$$

The above equation, which includes the parametric and forcing excitations, describes the nonlinear flexural oscillations of the in-plane and out-of-plane for the cantilever beam.

We use the method of multiple scales [53] to find the uniform solutions of Eq. (3.8) in the following form:

$$y(t, \varepsilon) = y_0(T_0, T_1) + \varepsilon y_1(T_0, T_1) + \cdots, \tag{3.9a}$$

$$z(t, \varepsilon) = z_0(T_0, T_1) + \varepsilon z_1(T_0, T_1) + \cdots, \tag{3.9b}$$

where $T_0 = t$, $T_1 = \varepsilon t$.

We investigate the case of the ratio $\beta_y = \omega_1^2 \approx 1/4$. In this case, there is the relation of 2:1 internal resonance for Eq. (3.8). In addition, principal parametric resonance–1/2 subharmonic resonance for the in-plane mode and fundamental parametric resonance–primary resonance for the out-of-plane mode are considered. The resonant relations are represented as

$$\Omega_1 = \Omega_2, \quad \omega_1^2 = \beta_y = \tfrac{1}{4}\Omega_1^2 + \varepsilon\sigma_1, \quad 1 = \omega_2^2 = \Omega_1^2 + \varepsilon\sigma_2, \tag{3.10}$$

where σ_1 and σ_2 are two detuning parameters. For convenience of the following analysis, let $\Omega_1 = 1$.

Substituting Eqs. (3.9) and (3.10) into Eq. (3.8), we obtain the averaged equation in the Cartesian form

$$\dot{x}_1 = -\tfrac{1}{2}cx_1 - (\sigma_1 + \alpha_1 F_1)x_2 + \tfrac{1}{16}(2\alpha_2 - 3\alpha_3)x_2(x_1^2 + x_2^2) - \beta_1 x_2(x_3^2 + x_4^2), \tag{3.11a}$$

$$\dot{x}_2 = (\sigma_1 - \alpha_1 F_1)x_1 - \tfrac{1}{2}cx_2 - \tfrac{1}{16}(2\alpha_2 - 3\alpha_3)x_1(x_1^2 + x_2^2) + \beta_1 x_1(x_3^2 + x_4^2), \tag{3.11b}$$

$$\dot{x}_3 = -\tfrac{1}{2}cx_3 - \tfrac{1}{2}\sigma_2 x_4 - \beta_2 x_4(x_1^2 + x_2^2) + \tfrac{1}{8}(2\alpha_2 - 3\alpha_3)x_4(x_3^2 + x_4^2), \tag{3.11c}$$

$$\dot{x}_4 = -\tfrac{1}{2}f_2 + \tfrac{1}{2}\sigma_2 x_3 - \tfrac{1}{2}cx_4 + \beta_2 x_3(x_1^2 + x_2^2) - \tfrac{1}{8}(2\alpha_2 - 3\alpha_3)x_3(x_3^2 + x_4^2), \tag{3.11d}$$

where $\beta_1 = (\alpha_3 + 3\alpha_4 - 9\alpha_5)/8$ and $\beta_2 = (4\alpha_3 - 3\alpha_4 - 9\alpha_5)/16$.

In order to reduce Eq. (3.11) and analyze the multi-pulse homoclinic and heteroclinic orbits and chaotic motions for the nonlinear non-planar oscillations of the cantilever beam, we will give normal form of averaged Eq. (3.11) using the Maple program developed by Zhang et al. [54]. The theory of normal form is one of the basic methods for the study of nonlinear dynamics such as the homoclinic and heteroclinic bifurcations. The theory of normal form is concerned with constructing a series of near identity nonlinear transformations that make the nonlinear systems as simple as possible. With the aid of normal form theory, we may obtain a set of simpler differential equations, which is topologically equivalent to the original systems.

It is observed that there are $Z_2 \oplus Z_2$ and D_4 symmetries in averaged Eq. (3.11) without the parameters. Therefore, these symmetries are also held in normal form. Take into account the exciting amplitude f_2 as a perturbation parameter. Amplitude f_2 can be considered as an unfolding parameter when the multi-pulse homoclinic and heteroclinic orbits are investigated. Obviously, when we do not consider the perturbation parameter, Eq. (3.11) becomes

$$\dot{x}_1 = -\tfrac{1}{2}cx_1 - (\sigma_1 + f_0)x_2 + \tfrac{1}{16}(2\alpha_2 - 3\alpha_3)x_2(x_1^2 + x_2^2) - \beta_1 x_2(x_3^2 + x_4^2), \tag{3.12a}$$

$$\dot{x}_2 = (\sigma_1 - f_0)x_1 - \tfrac{1}{2}cx_2 - \tfrac{1}{16}(2\alpha_2 - 3\alpha_3)x_1(x_1^2 + x_2^2) + \beta_1 x_1(x_3^2 + x_4^2), \tag{3.12b}$$

$$\dot{x}_3 = -\tfrac{1}{2}cx_3 - \tfrac{1}{2}\sigma_2 x_4 - \beta_2 x_4(x_1^2 + x_2^2) + \tfrac{1}{8}(2\alpha_2 - 3\alpha_3)x_4(x_3^2 + x_4^2), \tag{3.12c}$$

$$\dot{x}_4 = \tfrac{1}{2}\sigma_2 x_3 - \tfrac{1}{2}cx_4 + \beta_2 x_3(x_1^2 + x_2^2) - \tfrac{1}{8}(2\alpha_2 - 3\alpha_3)x_3(x_3^2 + x_4^2), \tag{3.12d}$$

where $f_0 = \alpha_1 F_1$.

It is obviously found that Eq. (3.12) has a trivial zero solution $(x_1, x_2, x_3, x_4) = (0, 0, 0, 0)$ at which the characteristic equation is of the form

$$\left(\lambda^2 + c\lambda + \tfrac{1}{4}c^2 + \sigma_1^2 - f_0^2\right)\left(\lambda^2 + c\lambda + \tfrac{1}{4}c^2 + \tfrac{1}{4}\sigma_2^2\right) = 0. \tag{3.13}$$

Let

$$\Delta_1 = \tfrac{1}{4}c^2 + \sigma_1^2 - f_0^2, \quad \Delta_2 = \tfrac{1}{4}(c^2 + \sigma_2^2). \tag{3.14}$$

When $c = 0$ and $\Delta_1 = \sigma_1^2 - f_0^2 = 0$ are simultaneously satisfied, system (3.12) has one double zero and a pair of pure imaginary eigenvalues

$$\lambda_{1,2} = 0, \quad \lambda_{3,4} = \pm i\bar{\omega}_2, \tag{3.15}$$

where $\bar{\omega}_2^2 = \sigma_2^2$.

Let $\sigma_1 = f_0 + \bar{\sigma}_1$ as well as set $f_0 = -1$ and consider $\bar{\sigma}_1$, c and f_2 as the perturbation parameters. Then, based on the aforementioned analysis given in Section 4 and executing the Maple program given by Zhang et al. [54],

three-order normal form of system (3.12) without the perturbation parameters is obtained as follows:

$$\dot{y}_1 = y_2, \tag{3.16a}$$

$$\dot{y}_2 = -\left(\tfrac{1}{8}\alpha_2 - \tfrac{3}{16}\alpha_3\right)y_1^3 + \beta_1 y_1 y_3^2 + \beta_1 y_1 y_4^2, \tag{3.16b}$$

$$\dot{y}_3 = -\tfrac{1}{2}\sigma_2 y_4 + \left(\tfrac{1}{4}\alpha_2 - \tfrac{3}{8}\alpha_3\right)y_4^3 - \beta_2 y_1^2 y_4 + \left(\tfrac{1}{4}\alpha_2 - \tfrac{3}{8}\alpha_3\right)y_3^2 y_4, \tag{3.16c}$$

$$\dot{y}_4 = \tfrac{1}{2}\sigma_2 y_3 - \left(\tfrac{1}{4}\alpha_2 - \tfrac{3}{8}\alpha_3\right)y_3^3 + \beta_2 y_1^2 y_3 - \left(\tfrac{1}{4}\alpha_2 - \tfrac{3}{8}\alpha_3\right)y_3 y_4^2. \tag{3.16d}$$

The results obtained above completely agree with those presented by using the direct method developed in [55]. Normal form with parameters can be written as

$$\dot{y}_1 = -\bar{\mu}y_1 + (1 - \sigma_1)y_2, \tag{3.17a}$$

$$\dot{y}_2 = \bar{\sigma}_1 y_1 - \bar{\mu}y_2 - \left(\tfrac{1}{8}\alpha_2 - \tfrac{3}{16}\alpha_3\right)y_1^3 + \beta_1 y_1 y_3^2 + \beta_1 y_1 y_4^2, \tag{3.17b}$$

$$\dot{y}_3 = -\bar{\mu}y_3 - \bar{\sigma}_2 y_4 + \left(\tfrac{1}{4}\alpha_2 - \tfrac{3}{8}\alpha_3\right)y_4^3 - \beta_2 y_1^2 y_4 + \left(\tfrac{1}{4}\alpha_2 - \tfrac{3}{8}\alpha_3\right)y_3^2 y_4, \tag{3.17c}$$

$$\dot{y}_4 = -\bar{f}_2 + \bar{\sigma}_2 y_3 - \bar{\mu}y_4 - \left(\tfrac{1}{4}\alpha_2 - \tfrac{3}{8}\alpha_3\right)y_3^3 + \beta_2 y_1^2 y_3 - \left(\tfrac{1}{4}\alpha_2 - \tfrac{3}{8}\alpha_3\right)y_3 y_4^2, \tag{3.17d}$$

where $\bar{\mu} = c/2$, $\bar{\sigma}_2 = \sigma_2/2$ and $\bar{f}_2 = f_2/2$.

Further, we let

$$y_3 = I\cos\gamma \quad \text{and} \quad y_4 = I\sin\gamma. \tag{3.18}$$

Substituting Eq. (3.18) into Eq. (3.17) yields

$$\dot{y}_1 = -\bar{\mu}y_1 + (1 - \bar{\sigma}_1)y_2, \tag{3.19a}$$

$$\dot{y}_2 = \bar{\sigma}_1 y_1 - \bar{\mu}y_2 - \left(\tfrac{1}{8}\alpha_2 - \tfrac{3}{16}\alpha_3\right)y_1^3 + \beta_1 y_1 I^2, \tag{3.19b}$$

$$\dot{I} = -\bar{\mu}I - \bar{f}_2 \sin\gamma, \tag{3.19c}$$

$$I\dot{\gamma} = \bar{\sigma}_2 I - \left(\tfrac{1}{4}\alpha_2 - \tfrac{3}{8}\alpha_3\right)I^3 + \beta_2 I y_1^2 - \bar{f}_2 \cos\gamma. \tag{3.19d}$$

In order to obtain the unfolding of Eq. (3.19), a linear transformation is introduced as

$$\begin{bmatrix} y_1 \\ y_2 \end{bmatrix} = \frac{\sqrt{|\beta_1|}}{\sqrt{|\beta_2|}} \begin{bmatrix} 1 - \bar{\sigma}_1 & 0 \\ \bar{\mu} & 1 \end{bmatrix} \begin{bmatrix} u_1 \\ u_2 \end{bmatrix}. \tag{3.20}$$

Then, we have

$$\begin{bmatrix} u_1 \\ u_2 \end{bmatrix} = \frac{\sqrt{|\beta_2|}}{\sqrt{|\beta_1|}(1 - \bar{\sigma}_1)} \begin{bmatrix} 1 & 0 \\ -\bar{\mu} & 1 - \bar{\sigma}_1 \end{bmatrix} \begin{bmatrix} y_1 \\ y_2 \end{bmatrix}. \tag{3.21}$$

Substituting Eqs. (3.20) and (3.21) into Eq. (3.19) and eliminating nonlinear terms which include the parameter $\bar{\sigma}_1$ yield the unfolding as follows:

$$\dot{u}_1 = u_2, \tag{3.22a}$$

$$\dot{u}_2 = -\mu_1 u_1 - \mu_2 u_2 + \eta_1 u_1^3 + \beta_1 u_1 I^2, \tag{3.22b}$$

$$\dot{I} = -\bar{\mu}I - \bar{f}_2 \sin\gamma, \tag{3.22c}$$

$$I\dot{\gamma} = \bar{\sigma}_2 I - \eta_2 I^3 + \beta_1 I u_1^2 - \bar{f}_2 \cos\gamma, \tag{3.22d}$$

where

$$\mu_1 = \bar{\mu}^2 - \bar{\sigma}_1(1 - \bar{\sigma}_1), \quad \mu_2 = 2\bar{\mu}, \quad \eta_1 = \frac{|\beta_1|}{|\beta_2|}\left(\frac{3}{16}\alpha_3 - \frac{1}{8}\alpha_2\right), \quad \eta_2 = \left(\frac{1}{4}\alpha_2 - \frac{3}{8}\alpha_3\right).$$

The scale transformations may be introduced as follows:

$$\mu_2 \to \varepsilon\mu_2, \quad \bar{\mu} \to \varepsilon\bar{\mu}, \quad \bar{f}_2 \to \varepsilon\bar{f}_2, \quad \eta_1 \to \eta_1, \quad \eta_2 \to \eta_2, \tag{3.23}$$

Then, normal form (3.22) can be rewritten as the form with the perturbations

$$\dot{u}_1 = \frac{\partial H}{\partial u_2} + \varepsilon g^{u_1} = u_2, \tag{3.24a}$$

$$\dot{u}_2 = -\frac{\partial H}{\partial u_1} + \varepsilon g^{u_2} = -\mu_1 u_1 + \eta_1 u_1^3 + \beta_1 u_1 I^2 - \varepsilon\mu_2 u_2, \tag{3.24b}$$

$$\dot{I} = \frac{\partial H}{\partial \gamma} + \varepsilon g^I - \varepsilon\bar{f}_2 \sin \gamma = -\varepsilon\bar{\mu}I - \varepsilon\bar{f}_2 \sin \gamma, \tag{3.24c}$$

$$I\dot{\gamma} = -\frac{\partial H}{\partial I} + \varepsilon g^\gamma - \varepsilon\bar{f}_2 \cos \gamma = \bar{\sigma}_2 I - \eta_2 I^3 + \beta_1 I u_1^2 - \varepsilon\bar{f}_2 \cos \gamma, \tag{3.24d}$$

where the Hamiltonian function H is of form

$$H(u_1, u_2, I, \gamma) = \tfrac{1}{2}u_2^2 + \tfrac{1}{2}\mu_1 u_1^2 - \tfrac{1}{4}\eta_1 u_1^4 - \tfrac{1}{2}\beta_1 I^2 u_1^2 - \tfrac{1}{2}\bar{\sigma}_2 I^2 + \tfrac{1}{4}\eta_2 I^4, \tag{3.25}$$

and g^{u_1}, g^{u_2}, g^I and g^γ are the perturbation terms induced by the dissipative effects

$$g^{u_1} = 0, \quad g^{u_2} = -\mu_2 u_2, \quad g^I = -\bar{\mu}I, \quad g^\gamma = 0. \tag{3.26}$$

4. Unperturbed dynamics of system

When $\varepsilon = 0$, it is noticed that system (3.24) is an uncoupled two-degree-of-freedom nonlinear system. The I variable appears in (u_1, u_2) components of system (3.24) as a parameter since $\dot{I} = 0$. Consider the first two decoupled equations

$$\dot{u}_1 = u_2, \tag{4.1a}$$

$$\dot{u}_2 = -\mu_1 u_1 + \eta_1 u_1^3 + \beta_1 I^2 u_1. \tag{4.1b}$$

When $\eta_I < 0$, system (4.1) can exhibit the homoclinic bifurcations. It is easy to see from Eq. (4.1) that when $\mu_1 - \beta_1 I^2 > 0$, the only solution of Eq. (4.1) is the trivial zero solution $(u_1, u_2) = (0, 0)$ which is the saddle point. On the curve defined by $\mu_1 = \beta_1 I^2$, that is,

$$\bar{\mu}^2 = \bar{\sigma}_1(1 - \bar{\sigma}_1) + \beta_1 I^2 \tag{4.2}$$

or

$$I_{1,2} = \pm\left[\frac{\bar{\mu}^2 - \bar{\sigma}_1(1 - \bar{\sigma}_1)}{\beta_1}\right]^{1/2}, \tag{4.3}$$

the trivial zero solution may bifurcate into three solutions through a pitchfork bifurcation, which are given by $q_0 = (0, 0)$ and $q_{\pm}(I) = (B, 0)$, respectively, where

$$B = \pm\left\{\frac{1}{\eta_1}[\bar{\mu}^2 - \bar{\sigma}_1(1 - \bar{\sigma}_1) - \beta_1 I^2]\right\}^{1/2}. \tag{4.4}$$

From the Jacobian matrix evaluated at the zero solution, it is known that the singular point q_0 are the saddle point. It is observed that the variables I and γ may actually represent the amplitude and phase of the nonlinear

vibrations. Therefore, we may assume that the relation $I \geqslant 0$ exists. Then, Eq. (4.3) becomes

$$I_1 = 0 \quad \text{and} \quad I_2 = \left[\frac{\bar{\mu}^2 - \bar{\sigma}_1(1 - \bar{\sigma}_1)}{\beta_1} \right]^{1/2}, \tag{4.5}$$

such that for all $I \in [I_1, I_2]$, unperturbed system (4.1) has one hyperbolic saddle point, q_0, which is connected to itself by a pair of homoclinic orbits, $u_{\pm}^h(T_1, I)$, that is, $\lim_{T_1 \to \pm\infty} u_{\pm}^h(T_1, I) = q_0(I)$.

Therefore, in full four-dimensional phase space the set defined by

$$M = \left\{ (u, I, \gamma) | u = q_0(0, 0), \quad I_1 \leqslant I \leqslant I_2, \quad 0 \leqslant \gamma \leqslant 2\pi \right\} \tag{4.6}$$

is a two-dimensional invariant manifold. From the results obtained in Section 2, it is known that two-dimensional invariant manifold M is normally hyperbolic. Two-dimensional normally hyperbolic invariant manifold M has three-dimensional stable and unstable manifolds, $W^s(M)$ and $W^u(M)$, respectively. The geometric structure of the stable and unstable manifolds of M in full four-dimensional phase space for the unperturbed system of Eq. (3.24) is given in Fig. 2.

The existence of the homoclinic orbits of system (4.1) to the saddle point $q_0(0, 0)$ indicates that the stable and unstable manifolds $W^s(M)$ and $W^u(M)$ intersect non-transversally along a three-dimensional homoclinic manifold denoted by X_0, which can be written as

$$X_0 = \left\{ (u, I, \gamma) | u = u_{\pm}^h(T_1, I), I_1 < I < I_2, \; \gamma = \int_0^{T_1} D_I H(u_{\pm}^h(T_1, I), I) \, ds + \gamma_0 \right\}. \tag{4.7}$$

Now we analyze the dynamics of the unperturbed system of Eq. (3.24) restricted to M. Considering the unperturbed system of Eq. (3.24) restricted to M yields

$$\dot{I} = 0, \tag{4.8a}$$

$$I\dot{\gamma} = D_I H(q_0, I), \quad I_1 \leqslant I \leqslant I_2, \tag{4.8b}$$
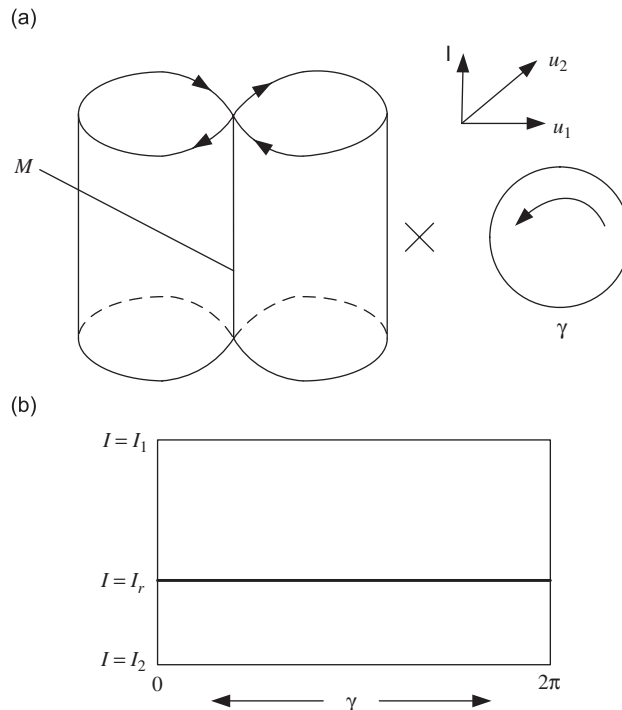
Fig. 2. The geometric structure of the manifolds M, $W^s(M)$ and $W^u(M)$ in full four-dimensional phase space.

where

$$D_I H(q_0, I) = -\frac{\partial H(q_0, I)}{\partial I} = \bar{\sigma}_2 I - \eta_2 I^3 + \beta_1 I q_0^2(I). \tag{4.9}$$

From the results obtained in Section 2, it is known that if $D_I H(q_0, I) \neq 0$ then $I = \text{constant}$ is called as a periodic orbit and if $D_I H(q_0, I) = 0$ then $I = \text{constant}$ is called as a circle of the singular points. A value of $I \in [I_1, I_2]$, at which $D_I H(q_0, I) = 0$ is satisfied, is called as a resonant I value and these singular points as resonant singular points. We denote a resonant value by I_r so that

$$D_I H(q_0, I) = \bar{\sigma}_2 I_r - \eta_2 I_r^3 + \beta_1 u_1^2 I_r = 0. \tag{4.10}$$

Then, we obtain

$$I_r = \pm \sqrt{\frac{\bar{\sigma}_2}{\eta_2}}. \tag{4.11}$$

Because the γ may represent the phase angle of the nonlinear oscillations, when $I = I_r$, the phase shift $\Delta\gamma$ of the nonlinear oscillations is defined as

$$\Delta\gamma = \gamma(+\infty, I_r) - \gamma(-\infty, I_r). \tag{4.12}$$

The physical interpretation of the phase shift is the phase difference between the two end points of the orbit. In (u_1, u_2) subspace, there exists a pair of homoclinic orbits connecting to the one saddle. Therefore, in fact the homoclinic orbit in (I, γ) subspace is of a heteroclinic connecting in full four-dimensional space (u_1, u_2, I, γ). The phase shift may denote the difference of γ value as a trajectory leaves and returns to the basin of attraction of M. We will use the phase shift in subsequent analysis to obtain the condition for the existence of the multi-pulse homoclinic orbits. The phase shift will be calculated in the later analysis given for the homoclinic orbit.

We consider the homoclinic orbits of system (4.1). Letting $\varepsilon_1 = -\mu_1 + \beta_1 \bar{I}^2$ and $\delta_1 = -\eta_1$, system (4.1) can be rewritten as

$$\dot{u}_1 = u_2, \quad \dot{u}_2 = \varepsilon_1 u_1 - \delta_1 u_1^3. \tag{4.13}$$

It is seen that system (4.13) is a Hamiltonian system with Hamiltonian

$$\bar{H}(u_1, u_2) = \tfrac{1}{2}u_2^2 - \tfrac{1}{2}\varepsilon_1 u_1^2 + \tfrac{1}{4}\delta_1 u_1^4. \tag{4.14}$$

When $\bar{H} = 0$, there exists a homoclinic loop Γ^0 which consists of one hyperbolic saddle point q_0 and a pair of homoclinic orbits $u_\pm(T_1)$. In order to calculate the phase shift, the extended Melnikov function and the energy difference function, we need to obtain the equations of a pair of homoclinc orbits which are given as

$$u_1(T_1) = \pm\sqrt{\frac{2\varepsilon_1}{\delta_1}}\mathrm{sech}\big(\sqrt{\varepsilon_1}T_1\big), \quad u_2(T_1) = \mp\frac{\sqrt{2}\varepsilon_1}{\sqrt{\delta_1}}\mathrm{th}\big(\sqrt{\varepsilon_1}T_1\big)\mathrm{sech}\big(\sqrt{\varepsilon_1}T_1\big). \tag{4.15}$$

Let us turn our attention to the computation of the phase shift. Substituting the first equation of Eq. (4.15) into the fourth equation of the unperturbed system of Eq. (3.24) yields

$$\dot{\gamma} = \bar{\sigma}_2 - \eta_2 I^2 + 2\beta_1 \frac{\varepsilon_1}{\delta_1}\mathrm{sech}^2\big(\sqrt{\varepsilon_1}T_1\big). \tag{4.16}$$

Integrating Eq. (4.16) yields

$$\gamma(T_1) = \omega_r T_1 + 2\beta_1 \frac{\sqrt{\varepsilon_1}}{\delta_1}\tanh\big(\sqrt{\varepsilon_1}T_1\big) + \gamma_0, \tag{4.17}$$

where $\omega_r = \bar{\sigma}_2 - \eta_2 I^2$.

At $I = I_r$, there is $\omega_r \equiv 0$. Therefore, the phase shift can be expressed as

$$\Delta\gamma = \left[\frac{4\beta_1\sqrt{\varepsilon_1}}{\delta_1}\right]_{I=I_r} = -\frac{4\beta_1}{\eta_1}\sqrt{\beta_1 I_r^2 - \bar{\mu}^2 + \bar{\sigma}_1(1 - \bar{\sigma}_1)}. \tag{4.18}$$

5. Existence of multi-pulse homoclinic orbits

After obtaining detailed information on the nonlinear dynamic characteristics of (u_1, u_2) components for the unperturbed system of Eq. (3.24) in Section 4, the next step is to examine the effects of small perturbation terms on the unperturbed system of Eq. (3.24). An extended Melnikov method developed by Camassa et al. [22] is utilized to discover the existence of the multi-pulse homoclinic orbits and chaotic dynamics for the nonlinear non-planar oscillations of the cantilever beam subjected to a harmonic axial excitation and two transverse excitations at the free end. We start by studying the influence of such small perturbations on the manifold M. The objective of research is to identify the parameter regions where the existence of the multi-pulse homoclinic orbits is possible in the perturbed phase space. It will be indicated that these multi-pulse homoclinic orbits can occur from the Hamiltonian system with the dissipative perturbations. The existence of such multi-pulse homoclinic orbits provides a robust mechanism for the existence of the complicated dynamics in the perturbed system. In this section, the emphasis is put on the application aspects of an extended Melnikov method to system (3.24).

5.1. Influence of dissipative perturbations

We analyze the dynamics of the perturbed system and the influence of small perturbations on M. Based on the analysis given in Section 2, it is known that M along with its stable and unstable manifolds $W^s(M)$ and $W^u(M)$ are invariant under small, sufficiently differentiable perturbations. It is noticed that the saddle-type singular point $q_0(I)$ may persist under small perturbations, in particular, $M \to M_\varepsilon$. We obtain

$$M = M_\varepsilon = \left\{ (u, I, \gamma) \big| u = q_0(0,0), I_1 \leqslant I \leqslant I_2, 0 \leqslant \gamma < 2\pi \right\}. \tag{5.1}$$

Considering the later two equations of system (3.22) yields

$$\dot{I} = -\bar{\mu}I - \bar{f}_2 \sin \gamma, \tag{5.2a}$$

$$\dot{\gamma} = \bar{\sigma}_2 - \eta_2 I^2 + \beta_1 u_1^2 - \frac{\bar{f}_2}{I} \cos \gamma. \tag{5.2b}$$

It is known from the aforementioned analysis that the last two equations of system (3.22) are of a pair of pure imaginary eigenvalues. Therefore, the resonance can occur in system (5.2). The scale transformations are also introduced as follows:

$$\bar{\mu} \to \varepsilon\bar{\mu}, \quad I = I_r + \sqrt{\varepsilon}h, \quad \bar{f}_2 \to \varepsilon\bar{f}_2, \quad T_1 \to T_1/\sqrt{\varepsilon}. \tag{5.3}$$

Substituting the above transformations into Eq. (5.2) yields

$$\dot{h} = -\bar{\mu}I_r - \bar{f}_2 \sin \gamma - \sqrt{\varepsilon}h\bar{\mu}, \tag{5.4a}$$

$$\dot{\gamma} = -2\eta_2 I_r h - \sqrt{\varepsilon}\left(\eta_2 h^2 + \frac{\bar{f}_2}{I_r}\cos \gamma \right). \tag{5.4b}$$

Because $0 < \varepsilon \ll 1$ is a small perturbation parameter, it is thought that the new time scale $\sqrt{\varepsilon}T_1$ in system (5.4) is a slow time. However, the time scale in system (4.1) is a fast time. When $\varepsilon = 0$, Eq. (5.4) becomes

$$\dot{h} = -\bar{\mu}I_r - \bar{f}_2 \sin \gamma, \tag{5.5a}$$

$$\dot{\gamma} = -2\eta_2 I_r h. \tag{5.5b}$$

The unperturbed system (5.5) is a Hamiltonian system with the Hamiltonian function

$$\hat{\mathrm{H}}_D(h, \gamma) = -\bar{\mu}I_r\gamma + \bar{f}_2 \cos \gamma + \eta_2 I_r h^2. \tag{5.6}$$

The singular points of system (5.5) are given as follows:

$$P_0 = (0, \gamma_c) = \left(0, -\arcsin[(\bar{\mu}I_r)/\bar{f}_2] \right), \tag{5.7}$$

$$Q_0 = (0, \gamma_s) = \left(0, \pi + \arcsin[(\bar{\mu}I_r)/\bar{f}_2] \right). \tag{5.8}$$

Based on the characteristic equations evaluated at the two singular points P_0 and Q_0, we can know the stabilities of these singular points. The characteristic equation corresponding to the singular point P_0 is obtained as

$$\lambda^2 - 2I_r\eta_2\bar{f}_2 \cos \gamma_c = 0. \tag{5.9}$$

When the condition $\left(2I_r\eta_2\bar{f}_2 \cos \gamma_c\right) < 0$ is satisfied, Eq. (5.5) has a pair of pure imaginary eigenvalues. Therefore, it is known that the singular point P_0 is a center.

The characteristic equation corresponding to the singular point Q_0 is obtained as

$$\lambda^2 - 2I_r\eta_2\bar{f}_2 \cos \gamma_s = 0. \tag{5.10}$$

When the condition $(2I_r\eta_2\bar{f}_2 \cos \gamma_s) > 0$ is satisfied, Eq. (5.5) has two real, unequal and opposite sign eigenvalues. Therefore, the singular point Q_0 is a saddle point which is connected to itself by a homoclinic orbit. The phase portrait of Eq. (5.5) is given in Fig. 3(a). It is found that for sufficiently small ε, the singular point Q_0 remains a hyperbolic singular point Q_ε of saddle stability type.

It is known that the Jacobian matrix of the linearization of Eq. (5.4) is of form

$$J_{p_\varepsilon} = \begin{bmatrix} -\sqrt{\varepsilon}\bar{\mu} & -\bar{f}_2 \cos \gamma_c \\ -2I_r\eta_2 & -\sqrt{\varepsilon}\bar{\mu} \end{bmatrix}. \tag{5.11}$$
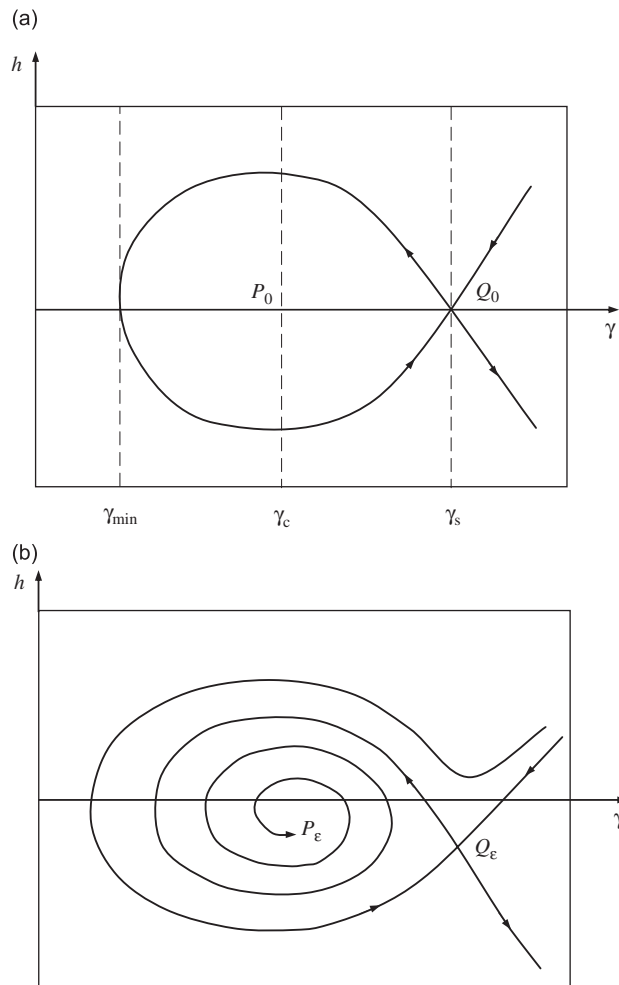
Fig. 3. Dynamics on the normally hyperbolic manifold: (a) the unperturbed case and (b) the perturbed case.

Based on Eq. (5.11), we find that the leading-order term of the trace in the linearization of Eq. (5.4) is less than zero inside the homoclinic loop. Therefore, for the small perturbations, the singular point P_0 becomes a hyperbolic sink P_ε. The phase portrait of perturbed system (5.4) is also depicted in Fig. 3(b).

At $h = 0$, the estimate of basin of attractor for $\gamma_{\min}$ is obtained as

$$-\bar{\mu} I_r \gamma_{\min} + \bar{f}_2 \cos \gamma_{\min} = -\bar{\mu} I_r \gamma_s + \bar{f}_2 \cos \gamma_s. \tag{5.12}$$

Substituting γ_s in Eq. (5.8) into Eq. (5.12) yields

$$\gamma_{\min} - \frac{\bar{f}_2}{\bar{\mu} I_r} \cos \gamma_{\min} = \pi + \arcsin \frac{\bar{\mu} I_r}{\bar{f}_2} + \frac{\sqrt{\bar{f}_2^2 - \bar{\mu}^2 I_r^2}}{\bar{\mu} I_r}. \tag{5.13}$$

Define an annulus A_ε near $I = I_r$ as

$$A_\varepsilon = \left\{ (u_1, u_2, I, \gamma) \big| u_1 = 0, u_2 = 0, |I - I_r| < \sqrt{\varepsilon} C, \gamma \in T^l \right\}, \tag{5.14}$$

where C is a constant, which is chosen sufficient large so that the unperturbed homoclinic orbit is enclosed within the annulus.

It is noticed that three-dimensional stable and unstable manifolds of the annulus A_ε, denoted as $W^s(A_\varepsilon)$ and $W^u(A_\varepsilon)$, are subsets of the manifolds $W^s(M_\varepsilon)$ and $W^u(M_\varepsilon)$, respectively. We will indicate that for the perturbed system, the saddle focus P_ε on A_ε has the multi-pulse heteroclinic jumping orbits which come out of the annulus A_ε and can return to the annulus in full four-dimensional space. These orbits, which are negatively asymptotic to some invariant manifolds in the slow manifold M_ε, leave and enter a small neighborhood of M_ε multiple times, and finally return and approach an invariant set in M_ε asymptotically, as shown in Fig. 4. In Fig. 4, three-pulse heteroclinic jumping orbit is depicted.

5.2. The k-pulse Melnikov function

We use an extended Melnikov method described in Section 2 to find the Shilnikov-type multi-pulse homoclinic orbits for the nonlinear non-planar oscillations of the cantilever beam. We reduce the search for the multi-pulse homoclinic excursions to that of finding non-degenerate zeros of an extended Melnikov function $M_k(\varepsilon, I, \gamma_0, \mu)$ with the certain parameters $\varepsilon, I, \gamma_0, \mu$, which we call as the k-pulse Melnikov function.

It is important to obtain the detailed expression of the k-pulse Melnikov function. First, we give the computation of 1-pulse Melnikov function based on Eq. (2.9) at the resonant case $I = I_r$. The 1-pulse Melnikov function $M(I, \gamma_0, \mu)$ on both homoclinic manifolds $W^s(M)$ and $W^u(M)$ is given as follows:

$$M(I_r, \gamma_0, \bar{\mu}, \beta_1, \delta_1, \varepsilon_1) = \int_{-\infty}^{+\infty} \langle n(p^h(t)), g(p^h(t), \mu, 0) \rangle \, dT_1 = \int_{-\infty}^{+\infty} \left(\frac{\partial H}{\partial u_1} g^{u_1} + \frac{\partial H}{\partial u_2} g^{u_2} + \frac{\partial H}{\partial I} g^I + \frac{\partial H}{\partial \gamma} g^\gamma \right) dT_1$$

$$= -\frac{4\mu_2}{3\delta_1} \varepsilon_1^{3/2} + 4\beta_1 \bar{\mu} I_r^2 \frac{\varepsilon_1^{1/2}}{\delta_1} - \bar{f}_2 I_r \left[\cos\left(\gamma_0 + 2\beta_1 \frac{\sqrt{\varepsilon_1}}{\delta_1} \right) - \cos\left(\gamma_0 - 2\beta_1 \frac{\sqrt{\varepsilon_1}}{\delta_1} \right) \right]. \tag{5.15}$$
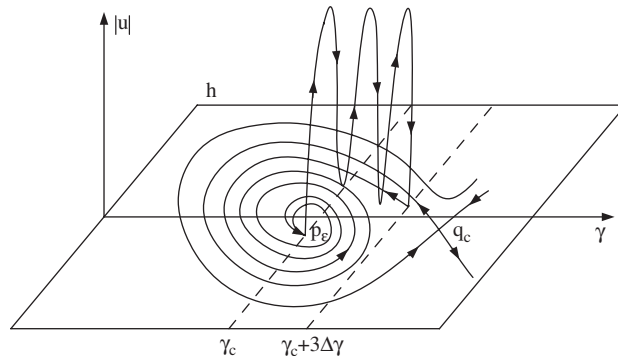
Fig. 4. The Shilnikov-type three-pulse heteroclinic jumping orbits to saddle focus.

When the resonance occurs, it is known form the aforementioned analysis given in Section 2 that there exist $\Gamma_j(\varepsilon, I_0, \gamma_0, \mu) = 0$, $(j = 0,1,\ldots,k-1)$. Based on Eq. (2.27), the k-pulse Melnikov function is obtained as follows:

$$
\begin{aligned}
M_k(I_r, \gamma_0, \bar{\mu}, \beta_1, \delta_1, \varepsilon_1) &= \sum_{j=0}^{k-1} M(I_r, \gamma_0 + j\Delta\gamma(I_r), \bar{\mu}, \beta_1, \delta_1, \varepsilon_1) \\
&= -\bar{f}_2 I_r \left[\cos\left(\gamma_0 + 2\beta_1 \frac{\sqrt{\varepsilon_1}}{\delta_1} \right) - \cos\left(\gamma_0 - 2\beta_1 \frac{\sqrt{\varepsilon_1}}{\delta_1} \right) \right] - \frac{4\mu_2}{3\delta_1} \varepsilon_1^{3/2} + 4\beta_1 \bar{\mu} I_r^2 \frac{\varepsilon_1^{1/2}}{\delta_1} \\
&\quad - \bar{f}_2 I_r \left[\cos\left(\gamma_0 + 2\beta_1 \frac{\sqrt{\varepsilon_1}}{\delta_1} + 4\beta_1 \frac{\sqrt{\varepsilon_1}}{\delta_1} \right) - \cos\left(\gamma_0 - 2\beta_1 \frac{\sqrt{\varepsilon_1}}{\delta_1} + 4\beta_1 \frac{\sqrt{\varepsilon_1}}{\delta_1} \right) \right] \\
&\quad - \frac{4\mu_2}{3\delta_1} \varepsilon_1^{3/2} + 4\beta_1 \bar{\mu} I_r^2 \frac{\varepsilon_1^{1/2}}{\delta_1} + \cdots - \bar{f}_2 I_r \left[\cos\left(\gamma_0 + 2\beta_1 \frac{\sqrt{\varepsilon_1}}{\delta_1} + (k-1)4\beta_1 \frac{\sqrt{\varepsilon_1}}{\delta_1} \right) \right. \\
&\quad \left. - \cos\left(\gamma_0 - 2\beta_1 \frac{\sqrt{\varepsilon_1}}{\delta_1} + (k-1)4\beta_1 \frac{\sqrt{\varepsilon_1}}{\delta_1} \right) \right] - \frac{4\mu_2}{3\delta_1} \varepsilon_1^{3/2} + 4\beta_1 \bar{\mu} I_r^2 \frac{\varepsilon_1^{1/2}}{\delta_1} \\
&= -\bar{f}_2 I_r \left[\cos\left(\gamma_0 + 2\beta_1 \frac{\sqrt{\varepsilon_1}}{\delta_1} + (k-1)4\beta_1 \frac{\sqrt{\varepsilon_1}}{\delta_1} \right) - \cos\left(\gamma_0 - 2\beta_1 \frac{\sqrt{\varepsilon_1}}{\delta_1} \right) \right] \\
&\quad - \frac{4k\mu_2}{3\delta_1} \varepsilon_1^{3/2} + 4k\beta_1 \bar{\mu} I_r^2 \frac{\varepsilon_1^{1/2}}{\delta_1}.
\end{aligned}
\tag{5.16}
$$

If we set $\Delta\gamma = (4\beta_1 \sqrt{\varepsilon_1})/\delta_1$ and $\gamma_{k-1} = \gamma_0 + [(k-1)\Delta\gamma]/2$, Eq. (5.16) can be rewritten as follows:

$$
\begin{aligned}
M_k(I_r, \gamma_0, \bar{\mu}, \beta_1, \delta_1, \varepsilon_1) &= M_k\left(I_r, \gamma_{k-1} - (k-1)\frac{\Delta\gamma}{2}, \bar{\mu}, \beta_1, \delta_1, \varepsilon_1 \right) \\
&= \bar{f}_2 I_r \left[\cos\left(\gamma_{k-1} - \frac{1}{2}k\Delta\gamma \right) - \cos\left(\gamma_{k-1} + \frac{1}{2}k\Delta\gamma \right) \right] - \frac{4k\mu_2}{3\delta_1} \varepsilon_1^{3/2} + 4k\beta_1 \bar{\mu} I_r^2 \frac{\varepsilon_1^{1/2}}{\delta_1} \\
&= 2\bar{f}_2 I_r \sin\gamma_{k-1} \sin\left(\frac{1}{2}k\Delta\gamma \right) - \frac{2\mu_2 \varepsilon_1}{3\beta_1}\left(\frac{1}{2}k\Delta\gamma \right) + 2\bar{\mu} I_r^2 \left(\frac{1}{2}k\Delta\gamma \right).
\end{aligned}
\tag{5.17}
$$

Based on Proposition 2.3 given in Section 2, the non-folding condition is always satisfied in the resonant case. We obtain the following two conditions:

$$
\left| \frac{(k\Delta\gamma)/2}{\sin[(k\Delta\gamma)/2]} \frac{(\mu_2 \varepsilon_1 - 3\beta_1 \bar{\mu} I_r^2)}{3\beta_1 \bar{f}_2 I_r} \right| < 1 \quad \text{and} \quad \frac{1}{2}k\Delta\gamma \neq n\pi, \quad n = 0, \pm 1, \pm 2, \ldots.
\tag{5.18}
$$

The main aim of the following analysis focuses on identifying simple zeroes of the k-pulse Melnikov function. Define a set that contains all such simple zeroes as

$$
Z_-^n = \left\{ (I_r, \gamma_{k-1}, \bar{\mu}, \beta_1, \delta_1, \varepsilon_1) \big| M_k = 0, \; D_{\gamma_0} M_k \neq 0 \right\}.
\tag{5.19}
$$

There are two simple zeroes of the k-pulse Melnikov function in the interval $\gamma_{k-1} \in [0, \pi]$

$$
\bar{\gamma}_{k-1,1} = \arcsin \frac{(k\Delta\gamma)/2}{\sin[(k\Delta\gamma)/2]} \frac{(\mu_2 \varepsilon_1 - 3\beta_1 \bar{\mu} I_r^2)}{(3\beta_1 \bar{f}_2 I_r)} \quad \text{and} \quad \bar{\gamma}_{k-1,2} = \pi - \bar{\gamma}_{k-1,1}.
\tag{5.20}
$$

Based on the aforementioned analysis, we obtain the following conclusions.

When the parameters k, μ_2, ε_1, $\bar{\mu}$, β_1, and $\bar{f}_2$ satisfy the condition (5.18), the k-pulse Melnikov function (5.17) has simple zeroes at some values γ_{k-1}, namely, at $\gamma_{k-1} = \bar{\gamma}_{k-1,1}$ and $\gamma_{k-1} = \bar{\gamma}_{k-1,2} = \pi - \bar{\gamma}_{k-1,1}$. For $i = 1$ or $i = 2$, when the j-pulse Melnikov function $M_j(I_r, \bar{\gamma}_{0,i}, \bar{\mu}, \beta_1, \delta_1, \varepsilon_1)$, with $\bar{\gamma}_{0,i} = \bar{\gamma}_{k-1,i} - (k-1)(\Delta\gamma/2)$ and $j = 1, \ldots, k-1$, where $j < k$, have no simple zeroes, then, the stable and unstable manifolds $W^s(M_\varepsilon)$ and $W^u(M_\varepsilon)$ intersect transversely along a symmetric pair of two-dimensional, k-pulse homoclinic surfaces $\sum_{\pm,\varepsilon}^{\bar{\mu},\beta_1,\delta_1,\varepsilon_1}(\bar{\gamma}_{k-1,i})$. This means that the presence of the n-pulse Shilnikov-type homoclinic orbits leads to chaotic dynamics in the sense of the Smale horseshoes for the nonlinear non-planar oscillations of the cantilever beam subjected to a harmonic axial excitation and two transverse excitations at the free end. In the phase space of the unperturbed

system of Eq. (3.24), this symmetric pair of two-dimensional, k-pulse homoclinic surfaces collapses smoothly onto a pair of limiting k-pulse surfaces, $\sum_{\pm,0}^{\bar{\mu},\beta_1,\delta_1,\varepsilon_1}(\bar{\gamma}_{k-1,i})$, parametrized by Eqs (4.15) and (4.17) with $I = I_r$, $\gamma_0 = \bar{\gamma}_{k-1,i} - (k-1)(\Delta\gamma/2) + j\Delta\gamma$, where $j = 1,\ldots,k-1$, and arbitrary h. The sign in Eq. (4.15) is determined by the sign of the corresponding j-pulse Melnikov function $M_j(I_r, \bar{\gamma}_{0,i}, \bar{\mu}, \beta_1, \delta_1, \varepsilon_1)$.

From the discussion in the previous sections, it is easily found that for $\bar{\gamma}_{0,i} = \bar{\gamma}_{k-1,i} - (k-1)(\Delta\gamma/2) + j\Delta\gamma$ ($i = 1$ or $i = 2$), the values of the j-pulse Melnikov functions $M_j(I_r, \bar{\gamma}_{0,i}, \bar{\mu}, \beta_1, \delta_1, \varepsilon_1)$ are not equal to zero for all $j = 1,\ldots,k-1$, where $j < k$, and are of the same sign for all j. It is known that this sign is negative for $\bar{\gamma}_{0,1}$ and positive for $\bar{\gamma}_{0,2}$. Therefore, the k-pulse homoclinic surfaces $\sum_{\pm,\varepsilon}^{\bar{\mu},\beta_1,\delta_1,\varepsilon_1}(\bar{\gamma}_{k-1,1})$ and $\sum_{\pm,\varepsilon}^{\bar{\mu},\beta_1,\delta_1,\varepsilon_1}(\bar{\gamma}_{k-1,2})$ indeed exist in this case for all k, and the limiting k-pulse surfaces, $\sum_{\pm,0}^{\bar{\mu},\beta_1,\delta_1,\varepsilon_1}(\bar{\gamma}_{k-1,1})$ and $\sum_{\pm,0}^{\bar{\mu},\beta_1,\delta_1,\varepsilon_1}(\bar{\gamma}_{k-1,2})$, also exist when $\varepsilon = 0$. Since the regions enclosed by the stable and unstable homoclinic manifolds $W^s(M)$ and $W^u(M)$ are both convex, and the normal $\mathbf{n} = ((-\mu_1 u_1 + \eta_1 u_1^3 + \beta_1 I^2 u_1), -u_2, 0, 0)$ is known to point out of these manifold, it is demonstrated that the orbits forming each of the surfaces $\sum_{\pm,0}^{\bar{\mu},\beta_1,\delta_1,\varepsilon_1}(\bar{\gamma}_{k-1,1})$ are parametrized by Eqs. (4.15) and (4.17) with alternating signs, and the orbits forming each of the surfaces $\sum_{\pm,0}^{\bar{\mu},\beta_1,\delta_1,\varepsilon_1}(\bar{\gamma}_{k-1,2})$ are parametrized by Eqs. (4.15) and (4.17) with the same signs.

For the parameter $\mu = \bar{\mu}$, there exist $N-1$ orbit segments $O_i(\bar{\mu})$ ($i = 2,\ldots,N$) on the annulus M, where the end points of the segments $O_i(\bar{\mu})$ are $d_i(\bar{\mu})$ and $c_i(\bar{\mu})$, respectively. The trajectories of system (5.5) on the segments $O_i(\bar{\mu})$ flow from the end points $d_i(\bar{\mu})$ to $c_i(\bar{\mu})$ in forward time. Therefore, the end points $d_i(\bar{\mu})$ and $c_i(\bar{\mu})$ are, respectively, referred to as the takeoff and landing points of the heteroclinic jumping Γ_i. In addition, the line $\gamma = \bar{\gamma}_{0,i}(I_r, \bar{\mu}) - \Delta\gamma^-(I_r)$ transversely intersects the segments $O_i(\bar{\mu})$ at the end point $c_i(\bar{\mu})$ for $i = 2,\ldots,N$. The line $\gamma = \bar{\gamma}_{0,i}(I_r, \bar{\mu}) + \Delta\gamma^+(I_r)$ transversely intersects the segments $O_{i+1}(\bar{\mu})$ at the end point $d_{i+1}(\bar{\mu})$ for $i = 1,\ldots,N-1$. For all $i = 2,\ldots,N-1$, the difference in the h coordinates of two end points $c_i(\bar{\mu})$ and $d_{i+1}(\bar{\mu})$ is equal to zero, namely

$$h(c_i(\bar{\mu})) - h(d_{i+1}(\bar{\mu})) = 0. \tag{5.21}$$

It is demonstrated that for each $i = 2,\ldots,N-1$, one of the heteroclinic orbits, which are represented by Γ_i and contained in the limiting surfaces $\sum_0^{\bar{\mu},\beta_1,\delta_1,\varepsilon_1}(\bar{\gamma}_{0,i})$ at the value $\mu = \bar{\mu}$, connects two intersection points $c_i(\bar{\mu})$ and $d_{i+1}(\bar{\mu})$. Therefore, a heteroclinic orbit Γ_1 on the limiting surfaces $\sum_0^{\bar{\mu},\beta_1,\delta_1,\varepsilon_1}(\bar{\gamma}_{0,1})$ connects the certain point $c_1(\bar{\mu})$ on the annulus M to the end point $d_2(\bar{\mu})$ on the segment $O_2(\bar{\mu})$. It is also known that a heteroclinic orbit Γ_N on the limiting surfaces $\sum_0^{\bar{\mu},\beta_1,\delta_1,\varepsilon_1}(\bar{\gamma}_{0,N})$ connects the end point $c_N(\bar{\mu})$ on the segments $O_N(\bar{\mu})$ to the certain point $d_{N+1}(\bar{\mu})$ on the annulus M. It is thought that there exists an n-bump singular transition orbit or a modified N-bump singular transition orbit [6,7,22]. Fig. 5 depicts the three-bump heteroclinic jumping orbit with the single-pulse. In Fig. 5, the three-bump homoclinic orbit with the single-pulse comprises the
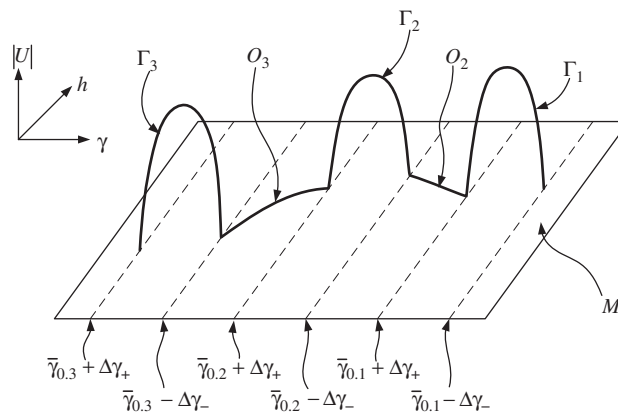
Fig. 5. The three-bump homoclinic orbit with the single-pulse is indicated.
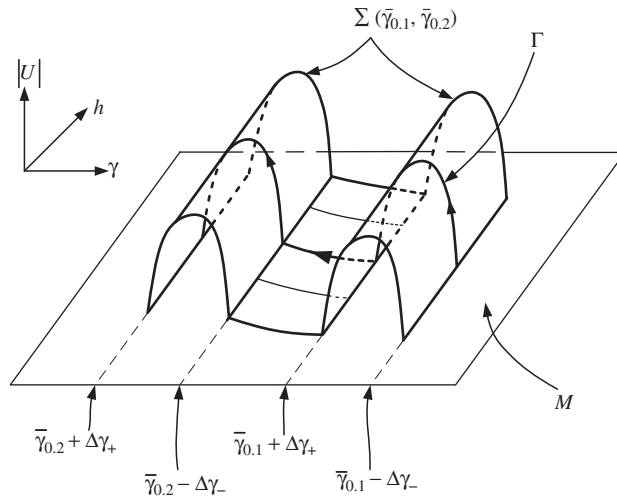
Fig. 6. The two-pulse homoclinic surfaces $\sum(\bar{\gamma}_{0,1}, \bar{\gamma}_{0,2})$ are depicted.

heteroclinic orbits Γ_i ($i = 1,2,3$) on the limiting surfaces $\sum_0^{\bar{\mu},\beta_1,\delta_1,\varepsilon_1}(\bar{\gamma}_{0,i})$ ($i = 1,2,3$) at the parameter $\mu = \bar{\mu}$ and the orbit segments $O_1(\bar{\mu})$ and $O_2(\bar{\mu})$ of (7.5). It is known from the above analysis that the orbit segments $O_i(\bar{\mu})$ ($i = 2,\ldots,N$) intersect transversely with the lines $\gamma = \bar{\gamma}_{0,i}(I_r, \bar{\mu}) + \Delta\gamma^+(I_r)$ and $\gamma = \bar{\gamma}_{0,i}(I_r, \bar{\mu}) - \Delta\gamma^-(I_r)$.

Fig. 6 illustrates the two-bump homoclinic surface, which is composed of two single-pulse singular intersection surfaces $\sum_0^{\bar{\mu},\beta_1,\delta_1,\varepsilon_1}(\bar{\gamma}_{k-1,1})$ and $\sum_0^{\bar{\mu},\beta_1,\delta_1,\varepsilon_1}(\bar{\gamma}_{k-1,2})$. This surface connects the singular points of Eq. (5.5) which lie on the line $\gamma = \bar{\gamma}_{0,1} - \Delta\gamma^-$ to those of system (5.5) which lie on the line $\gamma = \bar{\gamma}_{0,1} - \Delta\gamma^+$ on the annulus M.

We obtain a countable infinity of singular heteroclinic jumping orbits as follows. Each such orbit starts along one branch of the manifold $W(Q_0)$ of the saddle Q_0 on the annulus M. Then, the singular heteroclinic jumping orbit takes off from the annulus M along one of the singular k-pulse orbits Γ_k, and lands back on the annulus M at a point on the separatrix which connects the saddle Q_0 to itself. After running along the separatrix for a while, the singular heteroclinic jumping orbit again takes off along some singular l-pulse orbit Γ_l, and so forth. Eventually, the singular heteroclinic jumping orbit lands back on the separatrix.

Therefore, it is concluded that the multi-pulse homoclinic orbits of system (3.24) comprise several pieces of slow time on the hyperbolic manifold M_ε and many fast time heteroclinic pulses leaving from the manifold M_ε, which forms a consecutive and recurrence procedure.

6. Numerical results of chaotic motions

In this section, we will give numerical results of chaotic motions for the nonlinear non-planar oscillations of a cantilever beam. We choose averaged Eq. (3.11) to do numerical simulations. The Runge–Kutta algorithm is utilized to explore the existence of the multi-pulse chaotic motions.

Fig. 7 demonstrates the existence of the multi-pulse chaotic response for the nonlinear non-planar oscillations of the cantilever beam when $F_1 = 49.8$ and $f_2 = 416.8$. Other parameters and initial conditions are chosen as $c = 0.1$, $\sigma_1 = 2.0$, $\sigma_2 = 6.5$, $\alpha_1 = 1.0$, $\alpha_2 = 4.2$, $\alpha_3 = 0.01$, $\beta_1 = -5.1$, $\beta_2 = 2.3$, $x_{10} = 0.35$, $x_{20} = 0.180$, $x_{30} = 0.1385$, $x_{40} = 0.055$. Figs. 7(a)–(f), respectively, represent the phase portraits on the planes (x_1, x_2), (x_3, x_4), the waveforms on the planes (t, x_1), (t, x_3), the phase portraits in three-dimensional space (x_1, x_2, x_3), and the Poincare map on the plane (x_1, x_2).

In Fig. 8, the multi-pulse chaotic motion occurs when the axial excitation and transverse excitation in the z direction, respectively, are $F_1 = 49.8$, $f_2 = 416.8$, and parameters change to $c = 0.1$, $\sigma_1 = -2.0$, $\sigma_2 = 0.5$, $\alpha_1 = 1.0$, $\alpha_2 = -4.2$, $\alpha_3 = -1.1$, $\beta_1 = -5.1$, $\beta_2 = 0.23$. The initial conditions are $x_{10} = 0.35$, $x_{20} = 0.180$, $x_{30} = 0.1385$, $x_{40} = 0.055$. In comparison between the phase portraits in three-dimensional space (x_1, x_2, x_3)
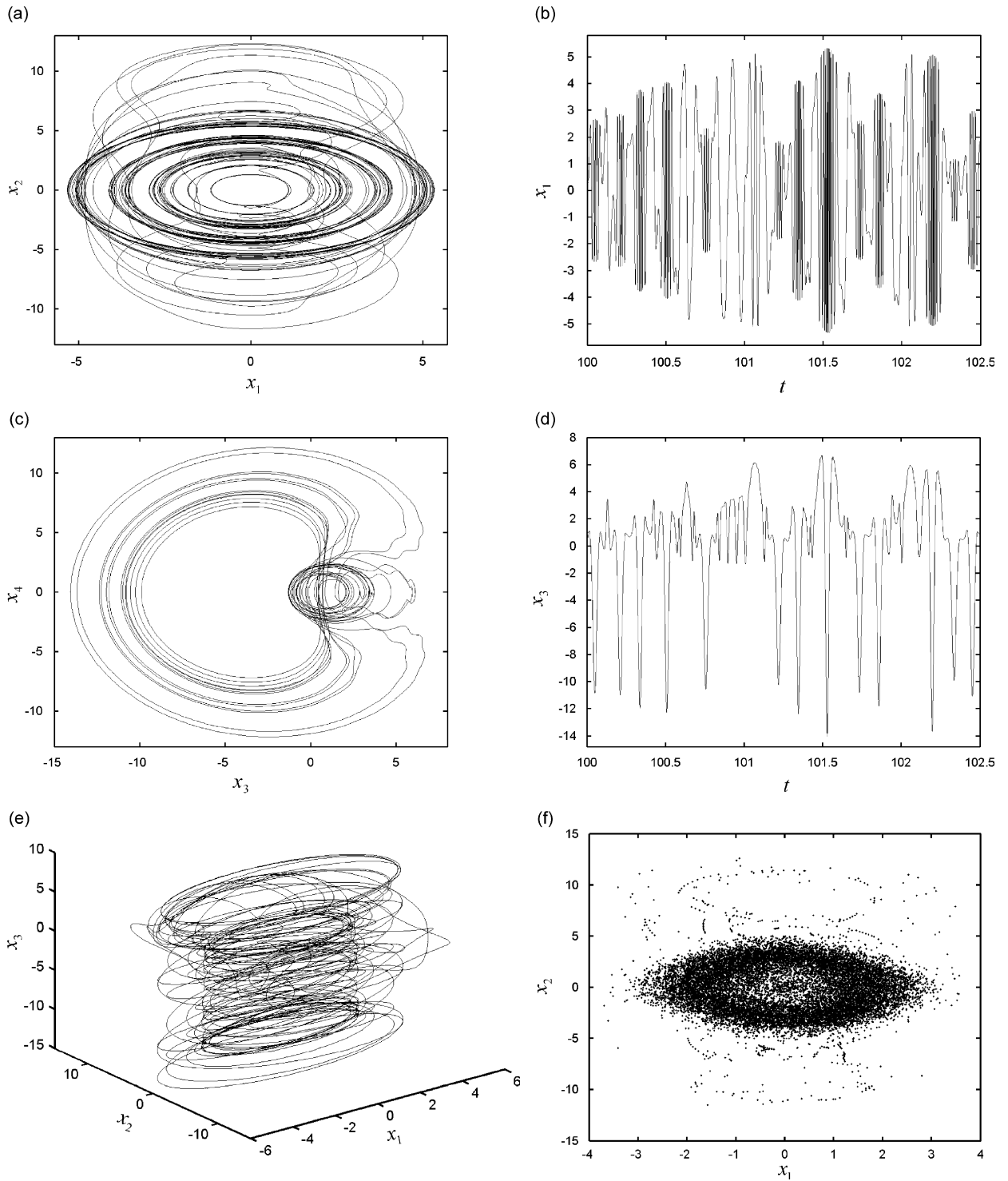
Fig. 7. The Shilnikov-type multi-pulse chaotic responses for the nonlinear non-planar oscillations of the cantilever beam for $F_1 = 49.8$, $f_2 = 416.8$, $c = 0.1$, $\sigma_1 = 2.0$, $\sigma_2 = 6.5$, $\alpha_1 = 1.0$, $\alpha_2 = 4.2$, $\alpha_3 = 0.01$, $\beta_1 = -5.1$, $\beta_2 = 2.3$, $x_{10} = 0.35$, $x_{20} = 0.180$, $x_{30} = 0.1385$, $x_{40} = 0.055$: (a) phase portrait on plane (x_1, x_2); (b) waveform on plane (t, x_1); (c) phase portrait on plane (x_3, x_4); (d) waveform on plane (t, x_3); (e) phase portraits in three-dimensional space (x_1, x_2, x_3) and (d) Poincare map on the plane (x_1, x_2).
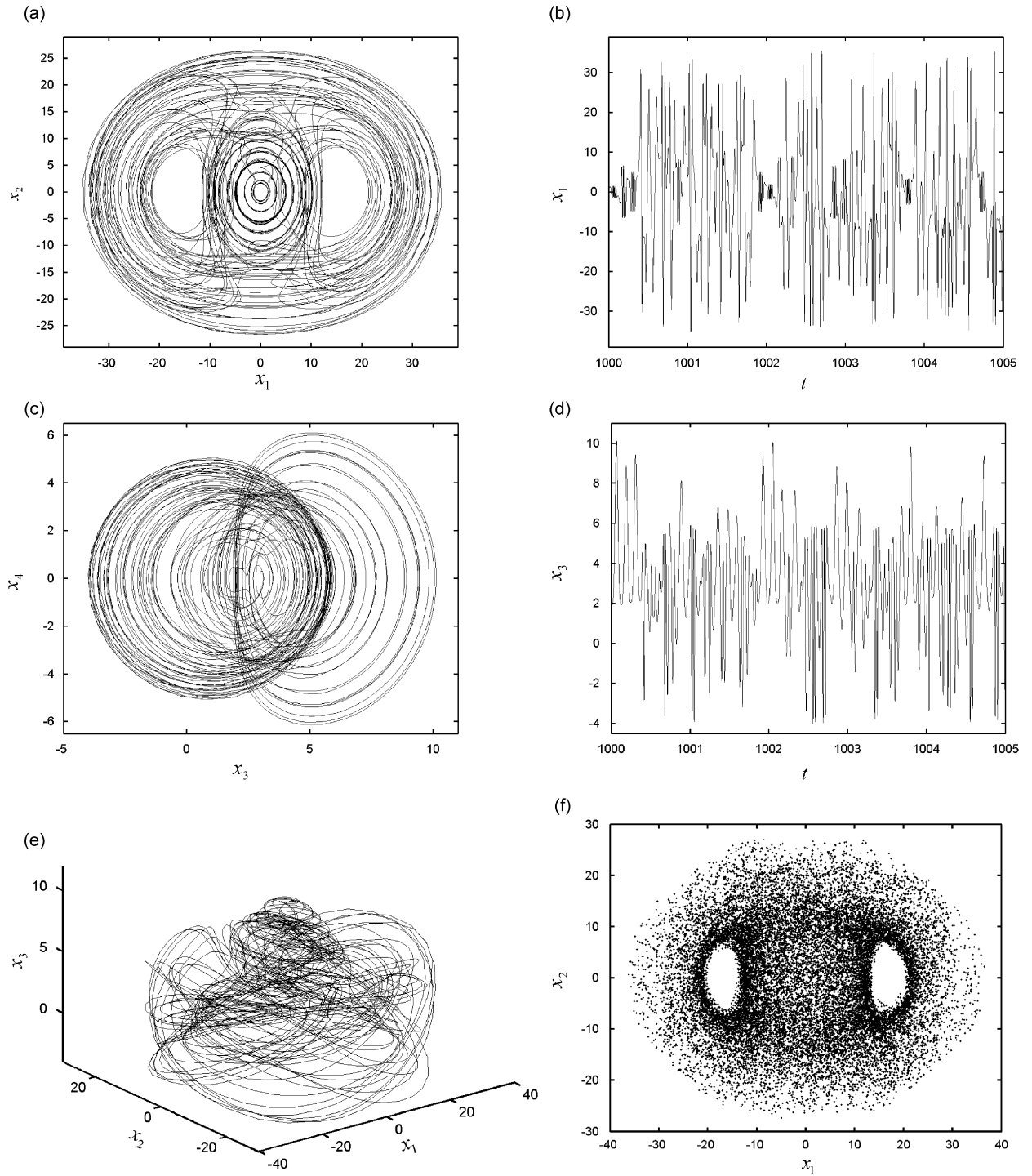
Fig. 8. The Shilnikov-type multi-pulse chaotic responses for the nonlinear non-planar oscillations of the cantilever beam for $F_1 = 49.8$, $f_2 = 416.8$, $c = 0.1$, $\sigma_1 = -2.0$, $\sigma_2 = 0.5$, $\alpha_1 = 1.0$; $\alpha_2 = -4.2$, $\alpha_3 = -1.1$, $\beta_1 = -5.1$, $\beta_2 = 0.23$, $x_{10} = 0.35$, $x_{20} = 0.180$, $x_{30} = 0.1385$, $x_{40} = 0.055$.
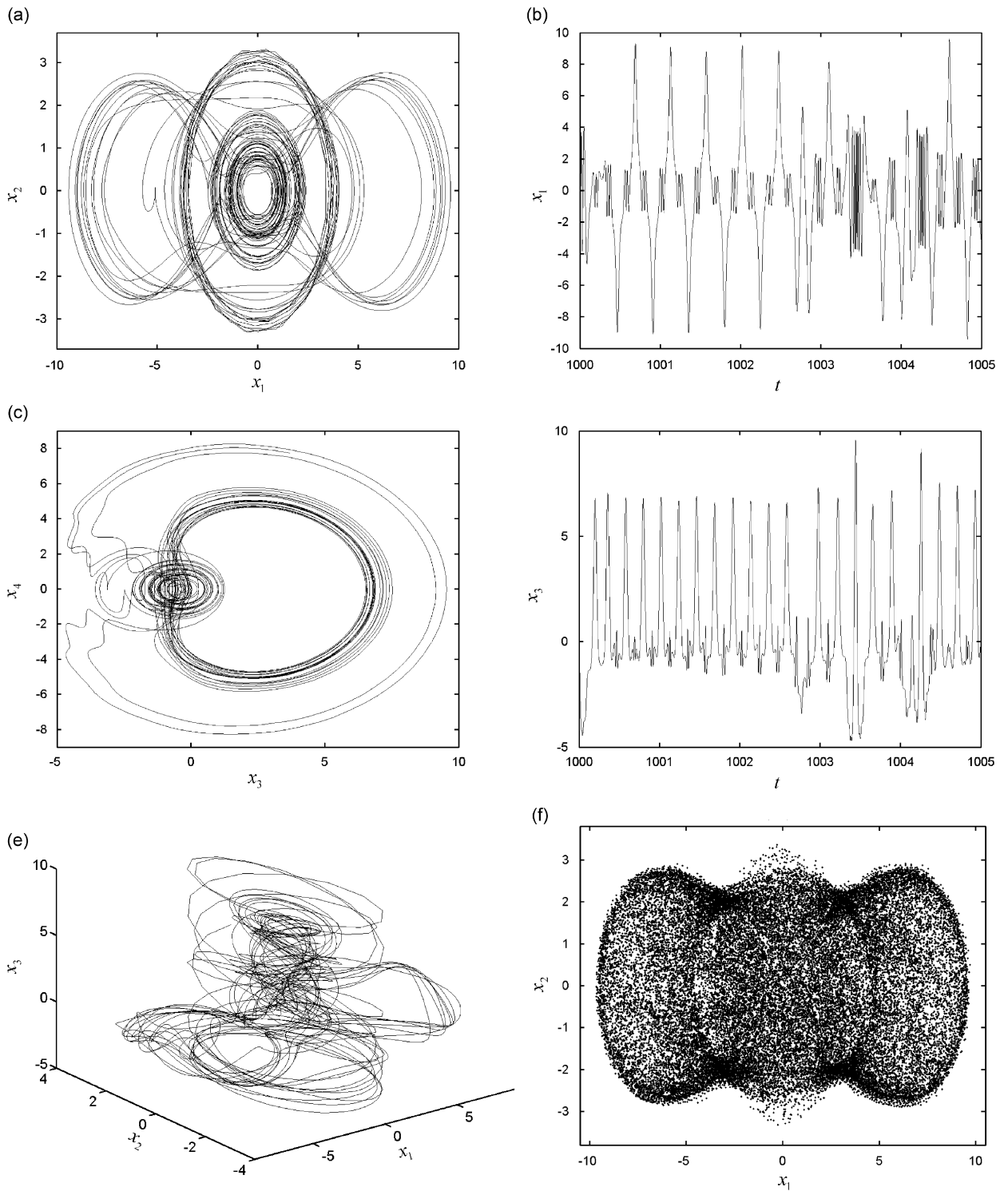
Fig. 9. The Shilnikov-type multi-pulse chaotic responses for the nonlinear non-planar oscillations of the cantilever beam for $F_1 = 48.4$, $f_2 = 198.4$, $c = 0.2$, $\sigma_1 = 11.4$, $\sigma_2 = 6.8$, $\alpha_1 = 1.0$, $\alpha_2 = -4.4$, $\alpha_3 = 1.1$, $\beta_1 = 4.9$, $\beta_2 = -3.9$, $x_{10} = 3.1385$, $x_{20} = 4.45$, $x_{30} = 4.35$, $x_{40} = 5.16$.

and the Poincare map for Figs. 7 and 8, it is found that there exists a large difference between them. Fig. 9 indicates that the multi-pulse chaotic response of the cantilever beam occurs when the axial excitation, transverse excitation in the z direction and the damping coefficient, respectively, are $F_1 = 48.4$, $f_2 = 198.4$, $c = 0.2$. Other parameters and the initial conditions in Fig. 9 are given as $\sigma_1 = 11.4$, $\sigma_2 = 6.8$, $\alpha_1 = 1.0$, $\sigma_2 = -4.4$, $\alpha_3 = 1.1$, $\beta_1 = 4.9$, $\beta_2 = -3.9$, $x_{10} = 3.1385$, $x_{20} = 4.45$, $x_{30} = 4.35$, $x_{40} = 5.16$. The shape of the phase portrait in three-dimensional space (x_1, x_2, x_3) for Figs. 7–9 indicates that the multi-pulse chaotic motions exist. The shape of the chaotic motions given by Figs. 7–9 is completely different.

7. Conclusions

In this paper, the main results on the theories of the multi-pulse global bifurcations and chaotic dynamics for high-dimensional nonlinear systems and their application to the nonlinear non-planar oscillations of the cantilever beam are given. The extended Melnikov method for studying the Shilnikov-type multi-pulse homoclinic and heteroclinic orbits and chaos in high-dimensional nonlinear systems is briefly introduced in the theoretical frame. The multi-pulse homoclinic orbits and chaotic dynamics for the nonlinear non-planar oscillations of the cantilever beam subjected to a harmonic axial excitation and two transverse excitations at the free end are investigated by using the extended Melnikov method when the averaged equations have one non-semisimple double zero and a pair of pure imaginary eigenvalues. This is a typical singular perturbation problem in which there are two different time scales, that is to say, the dynamics on the hyperbolic manifold M_ε is of slow time scale and the multi-pulse heteroclinic jumping orbits taking off from this manifold are of fast time scale. It can be conjectured that the transfer of energy between the in-plane and out-of-plane modes occurs through the Shilnikov-type multi-pulse heteroclinic jumping orbits. Through this example, we demonstrate how engineering researchers employ this method to analyze the Shilnikov-type multi-pulse homoclinic and heteroclinic bifurcations and chaotic dynamics of high-dimensional nonlinear systems in engineering applications.

The study on the nonlinear non-planar oscillations of the cantilever beam is focused on co-existence of 2:1 internal resonance, principal parametric resonance–1/2 subharmonic resonance for the in-plane mode and fundamental parametric resonance–primary resonance for the out-of-plane mode in Eq. (3.8). The existence of chaotic motions by identifying the existence of multi-pulse homoclinic orbits in the perturbed system is illustrated. In order to indicate the theoretical predictions, the Runge–Kutta algorithm is used to perform numerical simulation. The numerical results also show the existence of the multi-pulse chaotic motions in the averaged equations. It is well known that the multi-pulse chaotic motions in the averaged equations can lead to the multi-pulse amplitude-modulated chaotic oscillations in the original system under certain conditions. Therefore, it is demonstrated that there are the amplitude-modulated chaotic motions of the multi-pulse for the cantilever beam. We also find that the parametric excitation F_1, transverse excitation f_2 in the z direction and damping coefficient c have important influence on the multi-pulse chaotic motions for the nonlinear non-planar oscillations of the cantilever beam. Moreover, the aforementioned analysis also illustrates that the in-plane and out-of-plane nonlinear oscillations of the cantilever beam must be simultaneously considered when the in-plane and out-of-plane principal flexural stiffnesses are different, that is, $\beta_y = D_\varsigma / D_\eta \neq 1$.

The geometric interpretation of the k-pulse Melnikov function is a signed distance measured along the normal to a homoclinic or heteroclinic manifold, which replaces the estimate of the change of energy calculated along the unperturbed homoclinic or heteroclinic orbits. It is thought the construction of the energy-phase function developed in [23–25,28] employs the details of the geometry that depends on the dynamics along the hyperbolic manifold being slow, while the derivation of the k-pulse Melnikov function avoids these details and gives the more delicate local estimates near the hyperbolic manifold. Generally speaking, it is also thought that the energy-phase method is easily applied to engineering problems. However, in the resonant case, the k-pulse extended Melnikov function $M_k(I, \gamma_0, \bar{\mu})$ does not depend on the small parameter $0 < \varepsilon \ll 1$, and the non-folding condition is automatically satisfied, which leads to $\Gamma_j(\varepsilon, I_r, \gamma_0, \mu) = 0$ $(j = 0,1,\ldots,k-1)$. Therefore, we can simplify the computing procedure of the extended Melnikov function which becomes identical to the energy-phase function in the resonant case.

As the aforementioned analysis, from engineering and application view point, nowadays mathematical theories and methods on the multi-pulse homoclinic and heteroclinic orbits and chaotic dynamics of high-dimensional nonlinear systems, including the extended Melnikov method and the energy-phase method, can

not satisfy the practical requirement of research because of the complexity and variety of high-dimensional nonlinear systems in engineering and science. It is thought that the extended Melnikov method and the energy-phase method are too abstract and abstruse to understand and use for engineering scientists in applications. In addition, many mathematical theories and methods on the multi-pulse homoclinic and heteroclinic bifurcations and chaotic dynamics of high-dimensional nonlinear systems can not be directly utilized to engineering problems. Therefore, it is necessary for one to improve and develop these theories, such that we obtain suitable methods to investigate the multi-pulse homoclinic and heteroclinic bifurcations and chaotic dynamics of high-dimensional nonlinear system in many significant engineering problems.

Nowadays mathematical theories and methods on the global bifurcations and chaotic dynamics of high-dimensional nonlinear systems cannot satisfy the practical requirement of research because of the complexity and variety of high-dimensional nonlinear systems in engineering and science. Therefore, suitable methods need to be developed to investigate the global bifurcations and chaotic dynamics of high-dimensional nonlinear system based on many significant engineering problems.

Acknowledgments

References

[1] W. Zhang, M.H. Yao, Theories of multi-pulse global bifurcations for high dimensional systems and applications to cantilever beam—I: theories, *International Journal of Modern Physics B*, 2008, accepted for publication.

[2] W. Zhang, M.H. Yao, Theories of multi-pulse global bifurcations for high dimensional systems and applications to cantilever beam—II: applications, *International Journal of Modern Physics B*, 2008, accepted for publication.

[3] S. Wiggins, *Global Bifurcations and Chaos—Analytical Methods*, Springer, New York, 1988.

[4] G. Kovacic, S. Wiggins, Orbits homoclinic to resonance with an application to chaos in a model of the forced and damped sine-Gordon equation, *Physica D* 57 (1992) 185–225.

[5] G. Kovacic, Hamiltonian dynamics of orbits homoclinic to a resonance bands, *Physics Letters A* 167 (1992) 137–142.

[6] G. Kovacic, Singular perturbation theory for homoclinic orbits in a class of near-integrable Hamiltonian systems, *Journal of Dynamics and Differential Equations* 5 (1993) 559–597.

[7] G. Kovacic, Singular perturbation theory for homoclinic orbits in a class of near-integrable dissipative systems, *SIAM Journal on Mathematical Analysis* 26 (1995) 1611–1643.

[8] Z.C. Feng, S. Wiggins, On the existence of chaos in a parametrically forced mechanical systems with broken $O(2)$ symmetry, *Zeitschrift für Angewandte Mathematik und Physik (ZAMP)* 44 (1993) 201–248.

[9] Z.C. Feng, P.R. Sethna, Global bifurcations in the motion of parametrically excited thin plate, *Nonlinear Dynamics* 4 (1993) 389–408.

[10] N. Malhotra, N. Sri Namachchivaya, Global dynamics of parametrically excited nonlinear reversible systems with nonsemisimple 1:1 internal resonance, *Physica D* 89 (1995) 43–70.

[11] N. Malhotra, N. Sri Namachchivaya, Chaotic dynamics of shallow arch structures under 1:1 internal resonance, *ASCE Journal of Engineering Mechanics* 123 (1997) 620–627.

[12] Z.C. Feng, K.M. Liew, Global bifurcations in parametrically excited systems with zero-to-one internal resonance, *Nonlinear Dynamics* 21 (2000) 249–263.

[13] W. Zhang, Z.M. Liu, P. Yu, Global dynamics of a parametrically and externally excited thin plate, *Nonlinear Dynamics* 24 (2001) 245–268.

[14] W. Zhang, Global and chaotic dynamics for a parametrically excited thin plate, *Journal of Sound and Vibration* 239 (2001) 1013–1036.

[15] W. Zhang, J. Li, Global analysis for a nonlinear vibration absorber with fast and slow modes, *International Journal of Bifurcation and Chaos* 11 (2001) 2179–2194.

[16] W. Zhang, Y. Tang, Global dynamics of the cable under combined parametrical and external excitations, *International Journal of Non-Linear Mechanics* 37 (2002) 505–526.

[17] B.L. Guo, H.L. Chen, Homoclinic orbit in a six-dimensional model of a perturbed higher-order nonlinear Schrodinger equation, *Communications in Nonlinear Science and Numerical Simulation* 9 (2004) 431–441.

[18] W. Zhang, F.X. Wang, M.H. Yao, Global bifurcations and chaotic dynamics in nonlinear nonplanar oscillations of a parametrically excited cantilever beam, *Nonlinear Dynamics* 40 (2005) 251–279.

[19] D.X. Cao, W. Zhang, Global bifurcations and chaotic dynamics in a string-beam coupled system, *Chaos, Solitons and Fractals* 37 (2008) 858–875.

[20] G. Kovacic, T.A. Wettergren, Homoclinic orbits in the dynamics of resonantly driven coupled pendula, *Zeitschrift für Angewandte Mathematik und Physik (ZAMP)* 47 (1996) 221–264.

[21] T.J. Kaper, G. Kovacic, Multi-bump orbits homoclinic to resonance bands, *Transactions of the American Mathematical Society* 348 (1996) 3835–3887.

[22] R. Camassa, G. Kovacic, S.K. Tin, A Melnikov method for homoclinic orbits with many pulse, *Archive for Rational Mechanics and Analysis* 143 (1998) 105–119.

[23] G. Haller, S. Wiggins, Orbits homoclinic to resonance: the Hamiltonian, *Physica D* 66 (1993) 298–346.

[24] G. Haller, S. Wiggins, Multi-pulse jumping orbits and homoclinic trees in a modal truncation of the damped-forced nonlinear Schrodinger equation, *Physica D* 85 (1995) 311–347.

[25] G. Haller, S. Wiggins, N-pulse homoclinic orbits in perturbations of resonant Hamiltonian systems, *Archive for Rational Mechanics and Analysis* 130 (1995) 25–101.

[26] G. Haller, S. Wiggins, geometry and chaos near resonant equilibria of 3-DOF Hamiltonian systems, *Physica D* 90 (1995) 319–3657.

[27] G. Haller, Multi-dimensional homoclinic jumping and the discretized NLS equation, *Communications in Mathematical Physics* 193 (1998) 1–46.

[28] G. Haller, *Chaos Near Resonance*, Springer, New York, 1999.

[29] N. Malhotra, N. Sri Namachchivaya, R.J. McDonald, Multipulse orbits in the motion of flexible spinning discs, *Journal of Nonlinear Science* 12 (2002) 1–26.

[30] M.H. Yao, W. Zhang, Multi-pulse Shilnikov orbits and chaotic dynamics in nonlinear nonplanar motion of a cantilever beam, *International Journal of Bifurcation and Chaos* 15 (2005) 3923–3952.

[31] W. Zhang, M.H. Yao, Multi-pulse orbits and chaotic dynamics in motion of parametrically excited viscoelastic moving belt, *Chaos, Solitons and Fractals* 28 (2006) 42–66.

[32] M.H. Yao, W. Zhang, Shilnikov type multi-pulse orbits and chaotic dynamics of a parametrically and externally excited rectangular thin plate, *International Journal of Bifurcation and Chaos* 17 (2007) 851–875.

[33] O. De Feo, Qualitative resonance of Shilnikov-like strange attractors—part I: experimental evidence, *International Journal of Bifurcation and Chaos* 14 (2004) 873–891.

[34] O. De Feo, Qualitative resonance of Shilnikov-like strange attractors—part II: mathematical analysis, *International Journal of Bifurcation and Chaos* 14 (2004) 893–912.

[35] M.R.M. Crespo da Silva, C.C. Glynn, Nonlinear flexural–flexural torsional dynamics of inextensional beams, I: equation of motion, *Journal of Structural Mechanics* 6 (1978) 437–448.

[36] M.R.M. Crespo da Silva, C.C. Glynn, Nonlinear flexural–flexural torsional dynamics of inextensional beams, II: forced motions, *Journal of Structural Mechanics* 6 (1978) 449–461.

[37] M.R.M. Crespo da Silva, C.C. Glynn, Out-of-plane vibrations of a beam including nonlinear inertia and nonlinear curvature effects, *International Journal of Non-linear Mechanics* 13 (1979) 261–271.

[38] M.R.M. Crespo da Silva, C.C. Glynn, Nonlinear nonplanar resonant oscillations in fixed–free beams with support asymmetry, *International Journal of Solids and Structures* 15 (1979) 209–219.

[39] C.L. Zaretzky, M.R.M. Crespo da Silva, Experimental investigation of non-linear modal coupling in the response of cantilever beams, *Journal of Sound and Vibration* 174 (1994) 145–167.

[40] A.H. Nayfeh, P.F. Pai, Non-linear non-planar parametric responses of an inextensional beam, *International Journal of Non-linear Mechanics* 24 (1989) 139–158.

[41] P.F. Pai, A.H. Nayfeh, Non-linear non-planar oscillations of a cantilever beam under lateral base excitations, *International Journal of Non-linear Mechanics* 24 (1990) 455–474.

[42] J.P. Cusumano, F.C. Moon, Chaotic non-planar vibrations of the thin elastica—part I: experimental observation of planar instability, *Journal of Sound and Vibration* 179 (1995) 185–208.

[43] J.P. Cusumano, F.C. Moon, Chaotic non-planar vibrations of the thin elastica—part II: derivation and analysis of a low-dimensional model, *Journal of Sound and Vibration* 179 (1995) 209–226.

[44] T.J. Anderson, A.H. Nayfeh, B. Balachandran, Coupling between high-frequency modes and a low-frequency mode: theory and experiment, *Nonlinear Dynamics* 11 (1996) 17–36.

[45] H.N. Arafat, A.H. Nayfeh, C.M. Chin, Nonlinear nonplanar dynamics of parametrically excited cantilever beams, *Nonlinear Dynamics* 15 (1998) 31–61.

[46] E. Esmailzadeh, G. Nakhaie-Jazar, Periodic behavior of a cantilever beam with end mass subjected to harmonic base excitation, *International Journal of Non-linear Mechanics* 33 (1998) 567–577.

[47] M.N. Hamdan, A.A. Al-Qaisia, B.O. Al-Bedoor, Comparison of analytical techniques for nonlinear vibrations of a parametrically excited cantilever, *International Journal of Mechanical Sciences* 43 (2001) 1521–1542.

[48] S.A.Q. Siddiqui, M.F. Golnaraghi, G.R. Heppler, Large free vibrations of a beam carrying a moving mass, *International Journal of Non-linear Mechanics* 38 (2003) 1481–1493.

[49] P. Malatkar, A.H. Nayfeh, On the transfer of energy between widely spaced modes in structures, *Nonlinear Dynamics* 31 (2003) 225–242.

[50] S.K. Dwivedy, R.C. Kar, Simultaneous combination and 1:3:5 internal resonances in a parametrically excited beam-mass system, *International Journal of Non-Linear Mechanics* 38 (2003) 585–596.

[51] T.H. Young, C.S. Juan, Dynamic stability and response of fluttered beams subjected to random follower forces, *International Journal of Non-Linear Mechanics* 38 (2003) 889–901.

[52] W. Zhang, Chaotic motion and its control for nonlinear nonplanar oscillations of a parametrically excited cantilever beam, *Chaos, Solitons and Fractals* 26 (2005) 731–745.

[53] A.H. Nayfeh, D.T. Mook, *Nonlinear Oscillations*, Wiley-Interscience, New York, 1979.

[54] W. Zhang, F.X. Wang, J.W. Zu, Computation of normal forms for high dimensional non-linear systems and application to non-planar non-linear oscillations of a cantilever beam, *Journal of Sound and Vibration* 278 (2004) 949–974.

[55] P. Yu, W. Zhang, Q.S. Bi, Vibration analysis on a thin plate with the aid of computation of normal forms, *International Journal of Non-Linear Mechanics* 36 (2001) 597–627.